Advanced fingerprinting of high-quality cocoa: Challenges in transferring methods from thermal to differential-flow modulated comprehensive two dimensional gas chromatography

Advanced fingerprinting of high-quality cocoa: Challenges in transferring methods from thermal to differential-flow modulated comprehensive two dimensional gas chromatography

Federico Magagna[1], Erica Liberto[1], Stephen E. Reichenbach[2], Qingping Tao[3], Andrea Carretta[4], Luigi Cobelli[4], Matthew Giardina[4], Carlo Bicchi[1], Chiara Cordero[1*]

Authors' affiliation:

1 Università degli Studi di Torino Turin - Italy E-M@il: chiara.cordero@unito.it

2 University of Nebraska-Lincoln, NE, USA

3. GC Image, LLC, Lincoln NE, USA

4. SRA Intruments SpA, Cernusco sul Naviglio, Milan, Italy

5. Agilent Technologies, Wilmington DE, USA

* Address for correspondence:

Prof. Dr. Chiara Cordero - Dipartimento di Scienza e Tecnologia del Farmaco, Università di Torino, Via Pietro Giuria 9, I-10125 Torino, Italy – e-mail: chiara.cordero@unito.it ; phone: +39 011 6707662; fax: +39 011 2367662

Abstract

The possibility to transfer methods from thermal to differential-flow modulated comprehensive two-dimensional gas chromatographic (GC×GC) platforms opens interesting perspectives for routine analysis of complex samples. Flow modulated platforms avoid the use of cryogenics, thereby simplifying laboratory operations and analyst supervision during intensive analytical sessions.

This study evaluates the feasibility of transferring a fingerprinting method capable of classifying and discriminating cocoa samples based on the volatiles fraction composition according to their origin and processing steps. Previously developed principles of GC×GC method translation are applied to an original fingerprinting method, developed for a loop-type thermal modulated GC×GC-MS system, to engineer a method for a reverse-injection differential flow modulated platform (GC×2GC-MS/FID) with a dual-parallel secondary column and dual detection. Effective method translation preserves analytes elution order, ^{1}D resolution, and 2D pattern coherence.

The experimental results confirm the feasibility of translating fingerprinting method conditions while preserving the informative power of 2D peak patterns for sample classification and discrimination. Correct translation enables effective transfer of metadata (e.g., compound names and MS fragmentation patterns) by automatic template transformation and matching from the original/reference method to its translated counterpart. Although the adoption of a narrow bore (i.e. 0.1 mm d_c) column in the first-dimension enabled operation under close-to-optimal conditions with the differential-flow modulation platform, due to the dual-parallel columns in the second-dimension, it resulted in lower overall method sensitivity. Nevertheless, fingerprinting accuracy was preserved and most of the key-aroma compounds and technological markers were effectively mapped, thus limiting the loss of fingerprinting information.

Key-words:

comprehensive two-dimensional gas chromatography-mass spectrometry and flame ionization detection; reverse-inject differential flow modulation; advanced fingerprinting; *Theobroma cacao*; method translation; template matching functions

1. Introduction

Comprehensive two-dimensional gas chromatography (GC×GC) coupled with mass spectrometry (MS) has demonstrated great potentials for fingerprinting investigations in the field of complex food samples [1–4]. Fingerprinting is a common investigative approach adopted in metabolomics to discriminate and classify samples on the basis of a general, high-throughput screening, typically performed with rapid spectroscopic/spectrometric techniques (e.g., direct MS, Q-TOF, FT-ICR, MALDI, NMR, Raman, FT-IR etc)[5].

GC×GC offers unique possibilities for fingerprinting because it produces, for each sample, 2D patterns of separated analytes capable of explaining most of the sample chemical dimensionality [6]. This separation power derives from the combination of different retention mechanisms in the two chromatographic dimensions, which together provide ordered 2D patterns of analyte peaks. In addition, when mass spectrometry is used for detection, each sample's fingerprint acquires a further information dimension that is fundamental for analyte identification and quantitation.

The great potential of fingerprinting by GC×GC-MS is grounded in the highly detailed (bi-dimensional) profiles that do not require deconvolution and/or complex post-acquisition data manipulation to yield information about sample composition and/or key analytes [3,7–9].

Thermal modulated (TM) GC×GC platforms, implementing cryogenic cooling (liquid N_2, CO_2, or closed cycle refrigerator/heat exchangers) have been used widely for profiling volatiles and for fingerprinting studies of complex fractions from food. Effective cryogenic band focusing avoids breakthrough and preserves critical information for highly-volatile (C_2-C_4) compounds [10,11]. In addition, modulation parameters can be adapted to a sample's compositional characteristics. System loading capacity, modulation period (P_M), cold-jet temperature (obtained by varying the cold-jet volumetric flow per unit time), and hot-jet pulse temperature and duration can be tuned and optimized case-by-case with great flexibility. The main drawbacks of thermal modulation are relatively higher hardware and operational costs and complexity, factors which have limited wider adoption of GC×GC in quality control and high-throughput fingerprinting.

Differential-flow modulators (FMs), based on the device proposed by Seeley *et al.* [12–14] and successively modified for greater flexibility by Tranchida et al [15–17], are an interesting alternative to thermal modulators (TMs). FMs have a simple and effective design, limited operational and hardware costs, and high robustness. Commercially available devices were first introduced by Firor in 2006 [R.L. Firor, Application Brief 5989-6078EN, Agilent Technologies, 2007] utilizing a Capillary Flow Technology (CFT) microfluidic plate with forward fill/flush injection dynamics. FM GC×GC has been demonstrated for fatty acids methyl esters profiling from bacteria [18] and food samples [19], petrochemical analysis [20,21], and profiling of almonds volatiles [22].

A new generation of CFT plates (Agilent Technologies) is now available based on a reverse fill/flush (RFF) injection dynamic proposed by Griffith *et al.* [23]. These systems realize several advantages, including

efficient band re-injection, improved ^{2}D peak-widths and symmetry, and effective handling of collection-channel overloading. Results on system performances have been presented for different application fields, including fragrance formulations [23,24], heavy petroleum cuts [25], and medium-to-high complexity essential oils [26].

As a complement to a recent study on method translation for targeted quantitative profiling [24], the present investigation evaluates the feasibility of transferring fingerprinting applications from TM GC×GC-MS to FM platforms with dual-parallel secondary columns and detection: GC×2GC-MS/FID. Fingerprinting, if compared to profiling approaches, poses additional challenges due to the need of keeping 2D pattern informative and discriminative potential without any *a priori* knowledge on analytes identity. Based on the principles of method translation developed by Blumberg and Klee [27–30] for fast gas chromatography, an original method for origin traceability and processing qualification of high quality cocoa samples (*Theobroma cacao*, Trinitario hybrids) based on their volatile fraction 2D fingerprints was developed for TM GC×GC-MS and translated to a FM GC×2GC-MS/FID platform

This study addresses several challenges: (*a*) preservation of the informative content of 2D peak patterns by preserving the original method separation power and resolution; (*b*) generation of coherent 2D peak patterns between mutually translatable methods for a reliable transfer of metadata by automatic and/or supervised pattern recognition; and (*c*) fingerprinting accuracy of the FM GC×2GC-MS/FID translated method for reliable classification of samples according to origin and processing.

2. Experimental

2.1 Reference compounds, solvents, and cocoa samples

Pure standards of *n*-alkanes (from *n*-C9 to *n*-C25) for Linear Retention Indices ($\boldsymbol{I}^{T}_{s}$) calibration and of key-aroma compounds and informative volatiles for identity confirmation (acetic acid, 3-methyl butanoic acid, 3-methyl butanal, 2-phenyl ethanol, 2-heptanol, butanoic acid, 2-methyl butanal, linalool, phenylacetaldehyde, 2-ethyl-3,5-dimethyl pyrazine, 4-hydroxy-2,5-dimethyl-3(2H)-furanone (furaneol™), 2-ethyl-3,6-dimethyl pyrazine, (*E,E*)-2,4-nonadienal, dimethyl trisulfide, 2-methyl propanoic acid, and ethyl-2-methyl butanoate) were from Sigma-Aldrich (Milan, Italy).

The Internal Standard (ISTD) for response normalization (α-thujone) was from Fluka (Milan, Italy). The ISTD standard stock solution was prepared at a concentration of 1 µg/L in dibuthylphtalate (Sigma-Aldrich, Milan, Italy) and stored in a sealed vial at -18°C. Solvents (cyclohexane and toluene) were all HPLC-grade from Sigma-Aldrich (Milan, Italy).

Cocoa (*Theobroma cacao* L.) samples from Ecuador (Trinitario hybrid) and Mexico (Trinitario hybrid from the Chontalpa region of Tabasco), harvested in 2015, were analyzed at different technological stages (raw beans, roasted, steamed, and nibs). Chontalpa is a top cocoa-producing region of Tabasco (about 67% of the Mexican production). The area has favorable growing conditions and is the recognized origin of the

Criolla variety. The main varieties now grown in Chontalpa are Forastero (also locally called Calabacillo), Trinitario (or Puntudo), and, to a very limited extent, Criollo. Cocoa from this region received the Slow Food Presidium recognition in 2007. After devastating floods in 2007, most of the cocoa production of the region was lost and financial solidarity projects have aimed to restore cocoa plantations and support local communities. The Presidium identified a small group of producers of organic cocoa who process it using traditional methods and then supported them to establish a quality standard and a fair and ethical market for this top quality cocoa. Samples were kindly supplied by Guido Gobino srl, Turin (Italy), who acts as technological partner in this ethical project.

2.2 Automated Head Space Solid Phase Microextration - sampling conditions

Automated HS-SPME sampling was performed using a MPS-2 multipurpose sampler (Gerstel, Mülheim a/d Ruhr, Germany) installed on the GC×GC-MS systems. SPME fibers, Divinylbenzene/Carboxen/ Polydimethyl siloxane (DVB/CAR/PDMS) d_f 50/30 µm - 2 cm, were from Supelco (Bellefonte, PA, USA). Fibers were conditioned before use as recommended by the manufacturer. The ISTD (α-thujone) used for peak response normalization was pre-loaded into SPME fiber before sampling by exposing the extraction device (e.g., the SPME fiber) to 5 µL of ISTD standard stock solution for 20 minutes at 50°C.

Cocoa samples were frozen before milling, using liquid nitrogen, to ensure homogeneous particle size distribution thus stored at -80°C until analyzed. Samples were exactly weighed (1.500 g) in headspace glass vials (20 mL) and submitted to headspace extraction for 40 minutes at 50°C.

The sampling temperature was carefully tuned to melt the cocoa butter and enable a homogeneous release of volatiles in the headspace. Analyses were run in triplicate over one-week of analyses. Experimental results on repeatability for $^{1}D\ t_R$, $^{2}D\ t_R$, and Normalized Volumes based on Chontalpa nibs are reported as supplementary material (**Supplementary Tables**).

2.3 GC×GC with loop-type thermal modulation: instrument set-up and analysis conditions

The TM GC×GC system had an Agilent 7890B GC, equipped with a Zoex two-stage KT 2004 loop thermal modulator (Zoex Corp., Houston TX, USA), and coupled to an Agilent 5975C fast quadrupole MS detector (Agilent, Little Falls, DE, USA) operating in EI mode at 70 eV and a fast Flame Ionization Detector (FID) detector. The GC transfer line was set at 280°C. The MS was tuned using the Autotune (*Atune*) option. The scan range was set to m/z 40-240 with a scanning rate of 12,500 amu/s to obtain a spectra generation frequency of 28 Hz.

Injections for I^{T}_{S} determination were carried out with the MPS-2 auto sampler under the following conditions: injection mode split, split ratio 1:40, injection volume 1 µL, and injector temperature 270°C.
Fiber thermal desorption into the GC injector port was under the following conditions: split/splitless injector in pulsed split mode, and split ratio 1:5. Column configurations, carrier gas settings, and oven

programming are reported in **Table 1**.

2.4 GC×GC with reverse-inject differential flow modulation: instrument set-up and analysis conditions

GC×GC analyses with reverse-injection differential FM were run with a GC-MS system consisting of an Agilent 7890B GC unit coupled to an Agilent 5977B HES (High Efficiency Source) fast quadrupole MS detector (Agilent, Little Falls, DE, USA) operating in EI mode at 70 eV and a fast FID detector. The GC transfer line was set at 280°C. The MS was tuned using the *HES Tune* option. The scan range was set to m/z 40-240 with a scanning rate of 20,000 amu/s to obtain a spectrum generation frequency of 38 Hz. The FID conditions were: base temperature 280°C, H_2 flow 40 mL/min, air flow 350 mL/min, make-up (N_2) 20 mL/min, and sampling frequency 200 Hz.

The system was equipped with a reverse-injection differential FM (**Supplementary Figure S1**) consisting of one CFT plate connected to a three-way solenoid valve that receives a controlled supply of carrier gas (helium) from an auxiliary electronic pressure control module (EPC). The CFT plate, graphically depicted in **Supplementary Figure S1** in loading stage (**A**) and injection stage (**B**), has three-ports for connections of the first and second dimension columns and bleed capillary. The collection channel is etched into the plate itself. A brief description of the modulation dynamics is reported in the Supplementary Figure S1 caption.

Fiber thermal desorption into the GC injector port was under the following conditions: split/splitless injector in pulsed split mode and split ratio 1:20. Column configurations, carrier gas settings, and oven programming are reported in **Table 1**.

2.5 Column set and connections

Table 1 summarizes the columns set adopted in the two systems as well as pressure settings (S/SL injector and Auxiliary EPC) and corresponding carrier gas (helium) volumetric flows and linear velocities. **Table 1** also reports the oven temperature programs. Connections between the CFT plate and the two secondary columns were by a three-way un-purged splitter (G3181B, Agilent, Little Falls, DE, USA) and deactivated silica capillaries were connected by deactivated ultimate unions (G3182-61580 Agilent, Little Falls, DE, USA). ^{1}D Sol-Gel Wax™ columns were from SGE (Ringwood, Australia); ^{2}D columns (OV1701) and deactivated capillaries were from Agilent - J&W (Little Falls, DE, USA).

2.6 Data acquisition and 2D data processing by *UT fingerprinting*

Data were acquired by Enhanced MassHunter (Agilent Technologies, Little Falls, DE, USA) and processed using GC Image® GC×GC Edition Software, Release 2.6 (GC Image, LLC, Lincoln NE, USA). Post processing used XLSTAT software ver. 2014 (Addinsoft, New York, NY USA).

*U*ntargeted and *T*argeted *fingerprinting* (*UT fingerprinting*) was performed by applying the

template matching strategy, introduced by Reichenbach et al. in 2009 [31]. It uses the patterns of 2D peaks' metadata (retention times, MS fragmentation patterns, and detector responses) to establish reliable correspondences between the same chemical entities across multiple chromatograms. The output of template matching fingerprinting is a data matrix of aligned 2D peaks and/or peak-regions, together with their related metadata (^{1}D and ^{2}D retention times, compound names for target analytes, fragmentation patterns, single ion or total ion responses, etc.), that can be used for comparative purposes.

Targeted analysis focused on 132 selected compounds, each reliably identified by matching EI-MS fragmentation pattern (NIST MS Search algorithm, ver 2.0, National Institute of Standards and Technology, Gaithersburg, MD, USA, with Direct Matching threshold 900 and Reverse Matching threshold 950) with those collected in commercial (NIST2014 and Wiley 7n) and in-house databases. As a further parameter to support reliable identification, Linear Retention Indices (I^T_S) were measured and experimental values compared with tabulated ones.

Untargeted analysis was based on a *peak-regions* features approach [7,32,33] and was performed automatically by GC Image Investigator™ R2.6 (GC-Image LLC, Lincoln NE, USA). The untargeted analysis included all *peak-regions* above the arbitrarily fixed peak response threshold of 5,000 counts together with target peaks from the previous step. This approach re-aligned the 24 chromatograms (independently processing TM and FM runs) using a set of *registration peaks*. The resulting data matrix was a 24 × 600 for the TM and 24 × 450 for the FM method [samples (2 origins × 4 processing steps × 3 analytical replicates) × reliable *peak-regions*). Response data from aligned 2D *peak-regions* were used for multivariate analysis (MVA) and results from both approaches cross-compared to those obtained from target peaks distributions. (See *Sections 3.2* and *3.3* for the discussion of results.)

Visual feature fingerprinting, performed as pair-wise image comparison, was used to observe the evolution of volatiles patterns across processing steps and was rendered with "colorized fuzzy ratio" mode [34]. The algorithm computes the difference at each data point between pairs of TICs; a data point is the output of the detector at a point in time. These differences are mapped into Hue-Intensity-Saturation (HIS) color space to create an image for visualizing the relative differences between image pairs in the retention-times plane. A detailed description of the output of visual feature fingerprinting is provided in *Section 3.1*.

3. Results and discussion

This study explores the feasibility of transferring a fingerprinting method based on the informative patterns of volatiles in *Theobroma cacao* samples from a platform consisting of a GC×GC-MS with TM to a platform with reverse-injection FM and two parallel ^{2}D columns with detection by MS and FID. In particular, the main interest is to verify if the informative features (target analytes or unknowns), whose peculiar quali-quantitative distribution is diagnostic to describe cocoa origin, manufacturing processes, and sensory quality, are preserved with their diagnostic power, thus confirming the effectiveness of the method

transfer.

The following sections illustrate the chemical complexity of the volatile fraction of top quality cocoa samples, as it is revealed by GC×GC-MS and TM, and discuss the evolution of 2D patterns (quali-quantitative changes) along the early stages of processing. The role of informative analytes (*key-aroma* compounds [35,36] and technological markers) is also tackled from the perspective of the higher level of information they play within the fingerprinting process.

Method translation from TM GC×GC-MS and to the FM platform is discussed, briefly illustrating some practical details. The effectiveness of fingerprinting is validated by cross-comparing classification results based on targeted and untargeted outputs from the two platforms. A short discussion is dedicated to the feasibility of transferring the fingerprinting process in non-translated conditions, emphasizing the fundamental role played by pattern matching algorithms capable of effectively transferring all metadata between methods.

3.1 Chemical signatures encrypted in cocoa volatiles

The effectiveness of GC×GC (increased peak capacity and chromatographic resolution) plays a fundamental role in the characterization of complex volatile fractions from processed foods [1–3,37]. Cocoa volatiles are an interesting test bench because of their high chemical dimensionality [6] related to the concurrent effects of microbial fermentation on raw beans and thermal and mechanical induced reactions during processing (roasting, steaming and grinding).

The first step of the research aimed to characterize the chemical complexity of cocoa volatiles by mapping known (targets) and unknowns with *UT fingerprinting* [9] (see *Section 2.6*). VOCs from top quality cocoa samples of Trinitario hybrid harvested in two different geographical areas (Ecuador and Chontalpa, Mexico) were analyzed by HS-SPME-TM-GC×GC-MS and the resulting 2D patterns were interpreted by combining untargeted and targeted patterns to achieve the most comprehensive fingerprinting (i.e., *UT fingerprinting* strategy).

Samples were from the different stages of transformation: (*a*) raw beans that had been fermented in the country of origin; (*b*) roasted beans industrially processed to develop an optimal flavor bouquet and color for chocolate production; (*c*) steamed beans submitted to debacterization with high-pressure steam injection at high temperature; and (*d*) cocoa nibs obtained after grinding and husks elimination. During these early steps, cocoa develops its flavor potential and VOCs carry information about fermentation, odor (*key-aroma* compounds distribution), and processing.

Analytes detected by TM-GC×GC-MS were reliably identified and a list of 132 informative volatiles is reported in **Table 2**, together with their absolute retention times (^1t_R min and ^2t_R sec), experimental I^T_S, odor descriptors, and descriptive roles. They include potent odorants, analytes formed from non-volatile precursors thanks to the thermal transfer and/or hot water induced hydrolysis [35,36,38]

Figure 1 shows the evolution of the volatiles distribution along the manufacturing steps using visual-features fingerprinting [39]. In particular, raw cocoa originating from Chontalpa, Mexico, was taken as the reference pattern for comparative analysis with the successive stages: roasting, steaming, and grinding. These images picture the "colorized fuzzy ratio", which colors each pixel (corresponding to a single MS scan) in the retention-times plane. The algorithm computes the difference at each data point between aligned pair-wise images (each image normalized over the TIC response). In the regions colored in green, the difference is positive indicating that the relative response is higher in the analyzed image (A roasted, B steamed, and C nibs) whereas red pixels (negative difference) indicate a larger relative response in the reference image (raw cocoa). The intensity depends on the magnitude of the difference; white saturation indicates pixels at which peaks have nearly equal relative detector responses in the reference and analyzed image.

As illustrated by color maps, samples show significant differences in the distribution of volatiles across technological stages. In particular, after roasting, the volatile fraction becomes more complex (qualitative changes) and analytes that already were present in the fermented (raw) beans increase their relative abundance (predominance of green spots). Within all volatiles, the most relevant changes occur on *key-aroma* compounds and technological markers distribution, as confirmed by analyzing targeted analytes distribution across samples (**Table 2**).

Cocoa *key-aroma* markers, identified by Schieberle and his group [40,38,36], include several chemical classes: alkyl pyrazines (*2,3,5-trimethyl pyrazine*, *2-ethyl-3,5-dimethyl pyrazine* and *3,5-diethyl-2-methyl pyrazine*) are process markers with earthy notes; short chain and branched fatty acids (*acetic acid*, *butanoic acid*, *2-methyl propanoic acid* and *3-methyl butanoic acid*) above given thresholds can generate off-flavours due to their rancid, sour, and sweaty notes; Strecker aldehydes (*3-methylbutanal*), mostly formed during fermentation, have *malty* and *buttery* notes; and *phenylacetaldehyde*, derived from L-phenylalanine (L-Phe), is responsible for the pleasant *honey*-like note. Other key-markers are esters (*ethyl-2-methylbutanoate* – fruity, *2-phenyl ethyl acetate* – flowery), linear alcohols (*2-heptanol* – citrusy), phenyl propanoid derivates (*2-phenyl ethanol* – flowery), and sulfur derived compounds (*dimethyl trisulfide*).

Raw cocoa aroma is dominated by short chain fatty acids, especially *3-methyl butanoic* and *acetic acid*, formed by enzymatic degradation of the pulp during fermentation. A*cetic acid* is present at high levels in unroasted beans, giving an intense vinegar-like perception, but, after roasting, its concentration decreases by about 70% [36]. On the other hand, the major impact on aroma markers caused by the thermal treatment during roasting was observed for alkyl pyrazines and Strecker aldehydes. These two classes are chemically connected because Strecker aldehydes are also involved in pyrazines formation.

Roasting only slightly influences the level of the rancid smelling *3-methyl butanoic acid* and its esters, which are present in similar concentrations both in the unroasted and roasted beans.

In general, in cocoa, all *key-aroma* compounds are already present in raw (fermented) beans and they raise

up or modify their concentration after manufacturing process suggesting fermentation as the key step in the formation of cocoa flavor [41,42].

The distribution of known volatiles (132 known targets) was adopted for informative fingerprinting to discriminate samples with different characteristics (geographical origin and manufacturing stage).

An unsupervised multivariate approach, Principal Component Analysis (PCA), was applied to map the natural composition of sample sub-classes and to localize informative chemicals responsible for their differentiation. **Figure 2A** shows the scores plot on the first two principal components (F1-F2 plane), based on the 24 × 132 matrix (samples × targets) of the volatile fraction of cocoa samples from Chontalpa, Mexico (Ch), and Ecuador (Ec) at the four processing stages (R, raw; Ro, roasted; St, steamed; N, nibs). Autoscaling was applied as a pre-processing step and baseline correction was applied on 2D raw data during pre-processing by GC Image. The first principal component (F1) accounted for 41.27% of variance and the second PC (F2) accounted for 17.47%.

The PCA shows a clear clustering of cocoa samples based on the geographical origin along the first principal component (F1): cocoa samples from Ecuador are on the left side of the F1-F2 plane and samples from Chontalpa (Mexico) are on the right side. Moreover, a sub-division according to the stage of technological processing is evident along the second component (F2). In both cases, steamed beans and cocoa nibs are clustered together and well separated from raw and roasted samples. Volatiles from Ecuador and Mexico cocoas (both *Trinitario* hybrid) produce a clear and distinctive fingerprint that enables their independent clustering at most stages.

PCA loading plots, reported in tabular form in the Supplementary material - Supplementary Figure 2 and ranked according to the squared cosines of the variables on the F1 and F2 indicate analytes that contribute to the clustering: cocoa from Ecuador is characterized by a pool of short chain alcohols (*1-butanol*, *1-pentanol*, *1-hexanol*, *2-ethyl-1-hexanol*, *2-hexanol*, and *2-methyl-1-butanol*), linear aldehydes (*hexanal*, *octanal*, and *nonanal*), and fatty acids (C5-C9). These VOCs (linear and branched alcohols, acids) mostly derive from the fermentation process. In addition, the separation of steamed beans and nibs of Ecuador cocoa is driven by aromatic *ketones* such as *1-hydroxy-2-propanone*, *2,3-pentanedione*, *2,3-octanedione, 3-hydroxy-2-butanone*, and other compounds including *1H-pyrrole-2-carboxaldehyde*, *2-acetyl furane*, and *2-furan methanol*. In contrast to cocoa from Ecuador, the Chontalpa cocoa shows an intense and distinctive fingerprint of alkyl pyrazines (*2,3,5-trimethyl*, 2*,6-dimethyl*, *2,3-dimethyl*, *2-ethyl-3,5-dimethyl*, *2-ethyl-5(6)-methyl*, and *3,5-diethyl-2-methyl pyrazine*) and linear esters (e.g., *ethyl pentanoate*, *ethyl hexanoate*, *ethyl octanoate*, and *ethyl decanoate*). In addition, Chontalpa is characterized by a distinctive signature of some *key aroma* compounds*,* including a*cetic acid* (sour), *phenyl acetaldehyde* (honey-like), *2-phenyl ethanol* (flowery), phenyl propanoid derivates (*benzaldehyde* and *benzyl alcohol*), *3-methyl butanal* (malty), and *butanoic acid* (sweaty). On the other hand, the Ecuador aroma signature results from *2-heptanol* (citrusy), *3-methyl butanoic acid* (rancid), and *dimethyl trisulfide* (sulfurous).

To confirm the results observed by targeted fingerprinting, the investigation was extended to the entire pattern of detected VOCs (untargeted peak-regions). PCA results based on 595 reliable *peak-regions* (including the 132 targets) are visualized in **Figure 2B** and clearly confirm the consistency of clustering based on targeted analysis. In particular, the clustering based on untargeted compounds shows the same sub-divisions of cocoa samples on the basis of the geographical origin (Ecuador and Chontalpa, Mexico) along F1 and the influence of processing along F2. Results are coherent with the previous elaborations with a total explained variance of 62.81 % (F1 43.10%, F2 19.71 %).

Insights provided by Chontalpa cocoa fingerprinting are of interest for its quality valorization. Partial least squares discriminant analysis (PLS-DA) was adopted to find discriminant variables between known sub-classes of samples. Sub-classes were assigned according to the processing steps (raw, roasted, steamed and grinded) and the model was internally random cross-validated.. PLS-DA fits well with the data matrix characteristics having a high number of explanatory variables (targets) and few observations (sample sub-classes) although the risk of obtaining overfitting models in prediction would be high due to the limited representativeness of the sample set. Results on the quality of the classification model were good: confusion matrix for the estimation sample gave 100% of correctness for all classes and the cumulative R^2Y on the first three PCs was 0.968. The Variable Importance in Projection (VIP) on the first component (95% of confidence) indicates those variables with a higher informative role (along the F1) in discriminating samples classes. **Figure 3A** reports a histogram with the 20 most influential variables (cut-off of VIP>1) guiding the classification model. Within the 132 known analytes, the alkyl pyrazines group (*2-ethyl-6-methylpyrazine*, *2-ethyl-3,5-dimethyl-pyrazine*, 2-ethyl-5-methylpyrazine, *3,5-diethyl-2-methylpyrazine*, *2,3,5-trimethylpyrazine*, *2,6-dimethylpyrazine* and *2,3-dimethyl pyrazine*, and *methylpyrazine*) mostly differentiate raw *vs.* roasted and grinded cocoa samples. At the same time, some oxo-heterocycles, such as *furaneol*, *2-acetyl furane*, *acetyl pyrrole*, 2-furanmethanol, and *1H-pyrrole-2-carboxaldehyde*, vary along processing stages.

Steaming of roasted beans results in an informative variation of certain analytes, such as pyrazines, which enhance the earthy and roasty notes (*2-ethyl-5-methylpyrazine*, *2-ethyl-6-methylpyrazine*, *ethylpyrazine*, and *3,5-diethyl-2-methylpyrazine*); esters (*ethyl butanoate* and *hexyl acetate*); and ketones (*4-hydroxy-4-methyl-2-pentanone* and 2*,3-octanedione*). The high-pressure steam injection, useful for the reduction of the microbial count, enhances cellular permeability with the concurrent effect of the operative temperature on the release of volatiles and within them of some *key-aroma* compounds.

At the end of this explorative investigation and after having mapped the most informative analytes for an effective fingerprinting driven by origin and technological processing of samples, the study moved a step forward by evaluating the possibility to transfer the method to a FM platform.

3.2 Translation of the chromatographic method from thermal to differential flow modulated GC×GC

To transfer effectively the fingerprinting method from the TM-GC×GC-MS to the FM platform implementing dual-parallel secondary columns and detection (GC×2GC-MS/FID), the principles of method translation [27] for fast gas chromatography were applied. A detailed discussion on the principles and algorithms at the basis of this procedure are out of the scope of this paper but can be retrieved in reference studies by Blumberg and Klee [28–30].

This strategy previously was successful in transferring a quantitative profiling method for cosmetic fragrance allergens in raw materials [24]. However the sampling approach adopted (e.g., SPME) present some new challenges. With HS-SPME, volatiles are subjected to thermal-desorption at the injection port, this phenomenon affects the dynamics of analytes transfer into the ^{1}D column by increasing the length of the band entering into the column and producing a band-broadening in space. Cryogenic devices were not used to align the FM-GC×2GC-MS/FID platform with the needs of routine quality control. Therefore, transfer of highly volatile compounds from the SPME extraction fiber to the GC column becomes critical with ^{1}D narrow bore columns because of the relatively low carrier gas flow rates. However, a reliable transfer of the chromatographic conditions must: (*a*) preserve the ^{1}D elution order, peak capacity, and resolution of the original method; (*b*) generate coherent 2D peak patterns; and (*c*) transfer all features' metadata by automatic and/or supervised pattern recognition approaches. In the context of fingerprinting, preservation of the informative content of 2D peak patterns is fundamental to achieving the required accuracy for classification of samples.

The original separation method used a polar/medium-polarity column set consisting of a polyethylene glycol (PEG) stationary phase in the ^{1}D combined with 86% polydimethylsiloxane, 7% phenyl, 7% cyanopropyl in the ^{2}D. Based on the models developed by Blumberg and Klee [24,25,26,27] and implemented in patented software by Snyder and Blumberg [43], the original method settings were translated to a new method for the FM platform. Input parameters for method translation are reported in **Table 1** and include: ^{1}D column dimensions, inlet pressure (relative), outlet pressure (absolute), and carrier gas volumetric flow at the outlet of the ^{1}D column. Outlet pressure in the TM system corresponds to the midpoint pressure at the junction between the two dimensions. Calculations were based on reference equations [44] at a temperature of 40°C. Some translatable parameters were kept constant because of the fixed volume collection channel configuration: ^{1}D carrier gas volumetric flow was set at 0.3 mL/min (to avoid collection channel overloading during the loading state) and ^{1}D outlet pressure was set according to the requirement of providing about 12 mL/min volumetric flow at the outlet of ^{2}D parallel columns. With such ^{2}D flow, the modulation dynamics avoided trapping and breakthrough [23].

The translated parameters are reported in **Table 1**. Temperature programming was modified according to the estimated speed gain (G) and corresponding to the ratio between column void times ($t_{M\text{orig}}$ and $t_{M\text{tr}}$) while modulation period was reduced from 4 to 2 s. For the current application, G_{th} was expected to be 2.312 (40°C as reference temperature).

Figure 4 shows GC×GC images of a roasted Chontalpa sample analyzed with the original method on the loop-type TM platform (**4A**) and with the translated method by reverse-inject FM platform (**4B**). Pink circles indicate the positions of targeted peaks. The total analysis time for the translated method was reduced by a factor of 2, from 60 to about 30 minutes of analysis. The elution order was preserved as well as the relative positions of peaks in the second dimension. The consistency of the 2D pattern obtained facilitated the effective transfer of all metadata collected for targeted/untargeted (peak-regions) features in the original method (i.e., target peaks chemical names, reference MS, qualifier and quantifier ions, MS similarity thresholds, etc.) by template adaptation with global transformation algorithms [32,34,45].

3.3 Effective metadata transfer and fingerprinting accuracy on differential flow modulated GC×GC

The effective transfer of all metadata from all informative features (peaks or peak-regions) is fundamental for a successful method translation between GC×GC platforms. Metadata, and in particular those related to the relative positions of peaks (i.e., ^{1}D and ^{2}D retention times) and MS signatures (MS fragmentation patterns), are of primary importance for reliable fingerprinting operations and for preserving the chemical knowledge of sample composition. Constraints on MS fragmentation pattern similarity/identity evaluation, as well as limits on search in space within a user-defined time window in both dimensions, results in positive matches only for those analytes or features (unknowns) with coherent retention behavior and MS signature.

Second-degree polynomial global transformation algorithms [45,46] were applied to match all fingerprint features (targeted peaks and untargeted peak regions) from the original method to peak patterns obtained by translated conditions. The template matching process was supervised by scaling the template along the first dimension (Column I) by a factor that was inversely related to the speed gain G_{exp} (i.e., 0.5). Also, the ^{1}D absolute misalignment for the first peaks (related to the void time) was about 3 minutes, thus requiring a supervised global transformation of the template. In a second step, the template was adjusted on the second dimension retention space (Column II) and then matched on the actual peak pattern. The rescaled template was manually adjusted on early eluted peaks where the slow transfer to the ^{1}D column produced wider bands and critically resolved pairs. Finally, the procedure computes the second-degree polynomial function to fit the peak matches, and applies that transformation function to the whole template. These steps are illustrated graphically in the supplementary material (**Supplementary Figure 3**).

The template matching operation was performed on the MS detection channel to increase accuracy by requiring sufficient spectral similarity (NIST Algorithm). Reference spectra in the template objects were from original method by TM-GC×GC-MS with replicate analyses. Similarity thresholds were set to reduce false-negative matches as follows: Direct Match ≥ 700 and Reverse Match ≥ 700. Note, FM operates at higher ^{2}D volumetric flows compared to TM systems (about 5-6 mL/min instead of 1.3 mL/min), resulting in a sensitivity loss for MS detection because of the concurrent effect of differential-flow “dilution” and high

flow entering in the ion-source. In the FM-GC×GC platform, thanks to a highly effective ionization source, reliable spectra were obtained despite the high flow entering in the MS thereby facilitating template matching procedure [24].

Once adapted to the MS chromatogram, the template also was applied to the FID pattern where correspondences are established on relative peak positions with their neighbors. The misalignment between FID and MS traces was negligible (due to the different operative pressure between MS and FID detectors) and a small distance threshold was sufficient to match 100% of template objects (target peaks).

Untargeted fingerprinting based on peak-regions features deserve a separate discussion because its template, consisting of time-resolved/defined peak-regions, could not be effectively transformed and adapted to the translated pattern. This was mainly related to the different ^{1}D peak widths obtained by the two methods; the FM method with 0.10 mm d_c column, on average, halved ^{1}D peak-widths [24]. To overcome this issue and to develop a reliable untargeted template suited for mapping all pattern features, a feature template was automatically built to capture all peak patterns reliably. The resulting untargeted template (**Figure 4C)** built directly from the translated-method patterns from Chontalpa and Ecuador samples (24 runs) consisted of 140 reliable peaks (green circles) and 450 peak-regions (red graphics). Results, aligned in a data matrix, were compared to those deriving from the same procedure applied to the TM-GC×GC-MS analyses.

The translated methodology by FM-GC×2GC-MS/FID enabled mapping, on average, 54% of targeted peaks considering as reference benchmark those analytes revealed on the TM-GC×GC-MS patterns. Positive matches were for 57 target peaks from FM *vs*. 123 in the original method (TM) for Chontalpa raw beans, 71 *vs.* 123 for Chontalpa roasted beans, 68 *vs.* 122 for Chontalpa steamed and 70 *vs.* 125 for Chontalpa nibs.

The loss of fingerprinting sensitivity was expected due to the concurrent effect of: (*a*) limited ^{1}D column loadability (0.10 mm d_c *vs.* 0.25 mm d_c) that required higher split flows at the injection port to avoid peak overloading and streaking effects; (*b*) lack of band focusing in-space generally provided by cryogenic cooling at the injection stage; (c) splitting in two parallel ^{2}D columns to reduce carrier gas linear velocity and outlet flow toward the MS and ; (*d*) higher flow to the MS that impacts absolute detector sensitivity. However, targeted peak and peak-region (untargeted features) distributions were submitted to PCA to evaluate if this sensitivity loss was detrimental to the fingerprinting accuracy. Results on Ecuador and Chontalpa samples confirmed the clustering observed by TM platform (data not shown); the total explained variance by the first two components (F1 and F2) increased from 59% to 83% for the targeted approach and from 63% to 74% for the untargeted approach. PCA results suggest that the most informative variables for sample origin and technological treatments were effectively mapped by the FM methodology, thus preserving most of the intrinsic (chemical) information of the fingerprint.

PLS-DA was run to determine the most influential variables (cut-off of VIP>1) for Chontalpa cocoa samples along the processing steps. **Figure 3B** reports the first 20 variables within the 74 known analytes

cross-mapped over all samples (**Table 2**). Interestingly, most analytes highly influential in the TM-GC×GC fingerprinting were confirmed in their role, keeping also a coherent ranking (red bars in the histogram) within the first 20 VIPs.

To cross-validate fingerprinting results from both platforms and to confirm the reliability of the FM approach, a Multiple Factor Analysis (MFA) on the targeted peaks distribution was carried out. MFA makes it possible to analyze the two data matrix/tables (targeted peaks from TM and FM methods) simultaneously, and provides results capable of assessing the relationship between the observations (sample sub-classes) and the variables (targeted analytes). For each data matrix/table, PCA is performed first and the value of the first eigenvalue of each analysis is stored and then used to weight the two matrix/tables in a second step of the analysis. Results, expressed as RV coefficients, indicate to what extent the tables/variables distribution are related two-by-two. The more variables from the original method that are related to the variables of the translated counterpart, the higher the RV coefficient (variation range 0-1). In this case, the mutual correlation between the two data sets was 0.831 indicating a great consistency between fingerprints' informative content.

Graphical results in **Figure 5A** show the correlation between the factors obtained from the first phase of the MFA and those obtained from the second phase (after weighting) while **Figure 5B** displays the coordinates of the projected points in the space resulting from the MFA. The projected points correspond to projections of the observations in the spaces reduced to the dimensions of each table. The representation of the projected points superimposed on those of the complete observations makes it possible to visualize at the same time the diversity of the information brought by the two data sets corresponding to each sub-sample, and to visualize the relative distances. **Figure 5B** shows that the two data matrices are closely correlated and the relative position of the observations on the F1-F2 plane are coherently distributed.

Last, it should be stressed that, although the FM-GC×2GC-MS/FID method showed a lower fingerprinting sensitivity, the loss of chemical information was limited to analytes with an informing power not clearly correlated with sensory profile. Referring to *key-aroma* compounds described in previous studies, and evidenced in **Table 2**, the FM method maps 13 over 14 potent odorants. The one compound below the limit of detection (LoD) of the method is *phenyl acetaldehyde*.

3.4 Non translated conditions: challenges for template transformation algorithms

The original TM-GC×GC method also was adjusted for a FM-GC×GC platform not implementing a dual parallel secondary columns configuration and without translation of chromatographic conditions. This second approach for the FM platform adopts a common column configuration that affords low operative pressures and acceptable peak capacity [26]. The platform consisted of a conventional, 0.25 mm d_c column in the ^{1}D and a single ^{2}D column with the same internal diameter. A tee-splitter was used to divert the

effluent from the ^{2}D to parallel MS and FID detection. Column characteristics and operative conditions are reported in **Table 1**. This new column set does not suffer the limited sample loadability of the first FM system, but its carrier gas linear velocity in the ^{1}D is far from the ideal conditions. Chromatographic parameters were adjusted by trial-and-error to achieve the full chromatographic separation of target peaks while keeping modulation dynamics correct. The resulting 2D pattern is reported in **Figure 4D**. In this case, the temperature program was not normalized to the ^{1}D void time and P_M was kept at 3s.

The non-translated conditions did not significantly affect the 2D resolution; however, the analysis time increased of a factor of 1.75 (from 60 to 105 min). The elution order of some target analytes was not preserved, thus posing additional challenges for template transformation (**Figure 4D**).

With the non-translated method, the template adaptation was step-wise. Because of the severe misalignment of the two patterns, a minimal number of peaks were matched manually [45,47] to drive the global alignment for the template transform function. This effectively re-locates the position of the other/residual peaks with just a few matches. Again, the specificity of the matching was assured by forcing positive matches according to MS spectral similarity.

Results referring of fingerprint sensitivity are summarized in **Table 2**. Most analytes (103 target peaks) mapped by TM-GC×GC-MS also were positively matched by FM-GC×GC-MS/FID in non-translated mode although with lower system separation power.

4. Conclusions

This study confirms previous results on the feasibility of transferring applications from TM to differential FM-GC×GC-MS/FID platforms and extends the field of investigation strategies to advanced fingerprinting. In particular, experimental data on fingerprinting accuracy evaluated on a complex volatile fraction from cocoa, confirms that the effective translation of chromatographic parameters [27] produces 2D peak patterns that preserve their information potential, although a sensitivity loss is registered when 0.10 mm d_c columns are adopted in the ^{1}D. In addition, when 2D peak patterns are kept mutually coherent, the transfer of metadata (most importantly, compound names and MS fragmentation pattern) by template matching is effective and can be driven by few supervised operations followed by global second-order polynomial transformation.

The method translation and application transfer tasks were validated on a fingerprinting methodology aimed at classifying cocoa samples on the basis of their country of origin and processing steps. Fingerprinting accuracy, i.e., the coherent sub-classification of samples, was validated both on targeted and untargeted features and MVA methods were adopted to measure the degree of correlation between the results from the two platforms. The intrinsic information potential of samples' fingerprints also was analyzed in view of a sensory qualification of cocoa and, despite the loss of sensitivity for the translated FM-GC×2GC-MS/FID method, 13 over 14 key-aroma compounds were successfully detected.

The FM fingerprinting sensitivity when operating in non-translated conditions with conventional inner diameter columns (e.g., 0.25 mm d_c) is again comparable to that of the original TM method, but alterations of the elution order and 2D pattern inconsistencies pose challenging problems for template matching and metadata transfer.

Acknowledgments

Authors are indebted with Dr. Guido Gobino (Guido Gobino srl, Turin Italy) and Dr. Elena Allegrucci for precious advices and fruitful discussions.

References

[1] C. Cordero, C. Bicchi, P. Rubiolo, Group-type and fingerprint analysis of roasted food matrices (coffee and hazelnut samples) by comprehensive two-dimensional gas chromatography, J. Agric. Food Chem. 56 (2008) 7655–7666. doi:10.1021/jf801001z.

[2] C. Cordero, E. Liberto, C. Bicchi, P. Rubiolo, P. Schieberle, S.E. Reichenbach, Q. Tao, Profiling food volatiles by comprehensive two-dimensional ga schromatography coupled with mass spectrometry: Advanced fingerprinting approaches for comparative analysis of the volatile fraction of roasted hazelnuts (Corylus avellana L.) from different ori, J. Chromatogr. A. 1217 (2010) 5848–5858. doi:10.1016/j.chroma.2010.07.006.

[3] J. Kiefl, C. Cordero, L. Nicolotti, P. Schieberle, S.E. Reichenbach, C. Bicchi, Performance evaluation of non-targeted peak-based cross-sample analysis for comprehensive two-dimensional gas chromatography-mass spectrometry data and application to processed hazelnut profiling, J. Chromatogr. A. 1243 (2012) 81–90. doi:10.1016/j.chroma.2012.04.048.

[4] C. Cordero, J. Kiefl, P. Schieberle, S.E. Reichenbach, C. Bicchi, Comprehensive two-dimensional gas chromatography and food sensory properties: Potential and challenges, Anal. Bioanal. Chem. 407 (2015) 169–191. doi:10.1007/s00216-014-8248-z.

[5] J.M. Halket, D. Waterman, A.M. Przyborowska, R.K.P. Patel, P.D. Fraser, P.M. Bramley, Chemical derivatization and mass spectral libraries in metabolic profiling by GC/MS and LC/MS/MS, J. Exp. Bot. 56 (2005) 219–243. doi:10.1093/jxb/eri069.

[6] J.C. Giddings, Sample dimensionality: A predictor of order-disorder in component peak distribution in multidimensional separation, J. Chromatogr. A. 703 (1995) 3–15. doi:10.1016/0021-9673(95)00249-M.

[7] C. Cordero, E. Liberto, C. Bicchi, P. Rubiolo, S.E. Reichenbach, X. Tian, Q. Tao, Targeted and non-targeted approaches for complex natural sample profiling by GCxGC-qMS., J. Chromatogr. Sci. 48 (2010) 251–261. doi:10.1093/chromsci/48.4.251.

[8] G. Purcaro, C. Cordero, E. Liberto, C. Bicchi, L.S. Conte, Toward a definition of blueprint of virgin olive oil by comprehensive two-dimensional gas chromatography, J. Chromatogr. A. 1334 (2014) 101–111. doi:10.1016/j.chroma.2014.01.067.

[9] F. Magagna, L. Valverde-Som, C. Ruíz-Samblás, L. Cuadros-Rodríguez, S.E. Reichenbach, C. Bicchi, C. Cordero, Combined Untargeted and Targeted fingerprinting with comprehensive two-dimensional chromatography for volatiles and ripening indicators in olive oil, Anal. Chim. Acta. 936 (2016). doi:10.1016/j.aca.2016.07.005.

[10] C. Cordero, S.A. Zebelo, G. Gnavi, A. Griglione, C. Bicchi, M.E. Maffei, P. Rubiolo, HS-SPME-GC×GC-qMS volatile metabolite profiling of Chrysolina herbacea frass and Mentha spp. leaves, Anal. Bioanal. Chem. 402 (2012) 1941–1952. doi:10.1007/s00216-011-5600-4.

[11] J. Beens, M. Adahchour, R.J.J. Vreuls, K. Van Altena, U.A.T. Brinkman, Simple, non-moving modulation interface for comprehensive two-dimensional gas chromatography, J. Chromatogr. A. 919 (2001) 127–132. doi:10.1016/S0021-9673(01)00785-3.

[12] J. V. Seeley, N.J. Micyus, S. V. Bandurski, S.K. Seeley, J.D. McCurry, Microfluidic deans switch for comprehensive two-dimensional gas chromatography, Anal. Chem. 79 (2007) 1840–1847. doi:10.1021/ac061881g.

[13] J. V. Seeley, S.K. Seeley, Multidimensional gas chromatography: Fundamental advances and new applications, Anal. Chem. 85 (2013) 557–578. doi:10.1021/ac303195u.

[14] P.A. Bueno, J. V. Seeley, Flow-switching device for comprehensive two-dimensional gas chromatography, in: J. Chromatogr. A, 2004: pp. 3–10. doi:10.1016/j.chroma.2003.10.033.

[15] P.Q. Tranchida, F.A. Franchina, P. Dugo, L. Mondello, Flow-modulation low-pressure comprehensive two-dimensional gas chromatography, J. Chromatogr. A. 1372 (2014) 236–244. doi:10.1016/j.chroma.2014.10.097.

[16] P.Q. Tranchida, F.A. Franchina, P. Dugo, L. Mondello, Use of greatly-reduced gas flows in flow-modulated comprehensive two-dimensional gas chromatography-mass spectrometry, J. Chromatogr. A. 1359 (2014) 271–276. doi:10.1016/j.chroma.2014.07.054.

[17] P.Q. Tranchida, M. Maimone, F.A. Franchina, T.R. Bjerk, C.A. Zini, G. Purcaro, L. Mondello, Four-stage

(low-)flow modulation comprehensive gas chromatography-quadrupole mass spectrometry for the determination of recently-highlighted cosmetic allergens, J. Chromatogr. A. 1439 (2016) 144–151. doi:10.1016/j.chroma.2015.12.002.

[18] Q. Gu, F. David, F. Lynen, K. Rumpel, G. Xu, P. De Vos, P. Sandra, Analysis of bacterial fatty acids by flow modulated comprehensive two-dimensional gas chromatography with parallel flame ionization detector/mass spectrometry, J. Chromatogr. A. 1217 (2010) 4448–4453. doi:10.1016/j.chroma.2010.04.057.

[19] P. Manzano, E. Arnáiz, J.C. Diego, L. Toribio, C. García-Viguera, J.L. Bernal, J. Bernal, Comprehensive two-dimensional gas chromatography with capillary flow modulation to separate FAME isomers, J. Chromatogr. A. 1218 (2011) 4952–4959. doi:10.1016/j.chroma.2011.02.002.

[20] G. Semard, C. Gouin, J. Bourdet, N. Bord, V. Livadaris, Comparative study of differential flow and cryogenic modulators comprehensive two-dimensional gas chromatography systems for the detailed analysis of light cycle oil, J. Chromatogr. A. 1218 (2011) 3146–3152. doi:10.1016/j.chroma.2010.08.082.

[21] J. Krupčík, R. Gorovenko, I. Spánik, P. Sandra, D.W. Armstrong, Flow-modulated comprehensive two-dimensional gas chromatography with simultaneous flame ionization and quadrupole mass spectrometric detection., J. Chromatogr. A. 1280 (2013) 104–11. doi:10.1016/j.chroma.2013.01.015.

[22] J. Bernal, P. Manzano, J.C. Diego, J.L. Bernal, M.J. Nozal, Comprehensive two-dimensional gas chromatography coupled with static headspace sampling to analyze volatile compounds: Application to almonds, J. Sep. Sci. 37 (2014) 675–683. doi:10.1002/jssc.201301278.

[23] J.F. Griffith, W.L. Winniford, K. Sun, R. Edam, J.C. Luong, A reversed-flow differential flow modulator for comprehensive two-dimensional gas chromatography, J. Chromatogr. A. 1226 (2012) 116–123. doi:10.1016/j.chroma.2011.11.036.

[24] C. Cordero, P. Rubiolo, S.E. Reichenbach, A. Carretta, L. Cobelli, M. Giardina, C. Bicchi, Method translation and full metadata transfer from thermal to differential flow modulated comprehensive two dimensional gas chromatography: Profiling of suspected fragrance allergens, J. Chromatogr. A. (2016). doi:10.1016/j.chroma.2016.12.011.

[25] C. Duhamel, P. Cardinael, V. Peulon-Agasse, R. Firor, L. Pascaud, G. Semard-Jousset, P. Giusti, V. Livadaris, Comparison of cryogenic and differential flow (forward and reverse fill/flush) modulators and applications to the analysis of heavy petroleum cuts by high-temperature comprehensive gas chromatography, J. Chromatogr. A. 1387 (2015) 95–103. doi:10.1016/j.chroma.2015.01.095.

[26] C. Cordero, P. Rubiolo, L. Cobelli, G. Stani, A. Miliazza, M. Giardina, R. Firor, C. Bicchi, Potential of the reversed-inject differential flow modulator for comprehensive two-dimensional gas chromatography in the quantitative profiling and fingerprinting of essential oils of different complexity, J. Chromatogr. A. 1417 (2015) 79–95. doi:10.1016/j.chroma.2015.09.027.

[27] M.S. Klee, L.M. Blumberg, Theoretical and Practical Aspects of Fast Gas Chromatography and Method Translation, J. Chromatogr. Sci. 40 (2002) 234–247. doi:10.1093/chromsci/40.5.234.

[28] L.M. Blumberg, Theory of fast capillary gas chromatography. Part 1: Column efficiency, J. High Resolut. Chromatogr. 20 (1997) 597–604. doi:10.1002/jhrc.1240201106.

[29] L.M. Blumberg, Theory of fast capillary gas chromatography part. 2: Speed of analysis, J. High Resolut. Chromatogr. 20 (1997) 679–687. doi:10.1002/jhrc.1240201212.

[30] L.M. Blumberg, Theory of fast capillary gas chromatography - Part 3: Column performance vs. gas flow rate, HRC J. High Resolut. Chromatogr. 22 (1999) 403–413. doi:10.1002/(SICI)1521-4168(19990701)22:7<403::AID-JHRC403>3.0.CO;2-R.

[31] S.E. Reichenbach, P.W. Carr, D.R. Stoll, Q. Tao, Smart Templates for peak pattern matching with comprehensive two-dimensional liquid chromatography, 1216 (2009) 3458–3466. doi:10.1016/j.chroma.2008.09.058.

[32] S.E. Reichenbach, X. Tian, A.A. Boateng, C.A. Mullen, C. Cordero, Q. Tao, Reliable peak selection for multisample analysis with comprehensive two-dimensional chromatography, Anal. Chem. 85 (2013) 4974–4981. doi:10.1021/ac303773v.

[33] S.E. Reichenbach, X. Tian, Q. Tao, E.B. Ledford, Z. Wu, O. Fiehn, Informatics for cross-sample analysis with comprehensive two-dimensional gas chromatography and high-resolution mass spectrometry

(GCxGC-HRMS), Talanta. 83 (2011) 1279–1288. doi:10.1016/j.talanta.2010.09.057.
[34] B. V. Hollingsworth, S.E. Reichenbach, Q. Tao, A. Visvanathan, Comparative visualization for comprehensive two-dimensional gas chromatography, in: 2006: pp. 51–58. doi:10.1016/j.chroma.2005.11.074.
[35] P. Schnermann, P. Schieberle, Evaluation of Key Odorants in Milk Chocolate and Cocoa Mass by Aroma Extract Dilution Analyses, J. Agric. Food Chem. 45 (1997) 867–872. doi:10.1021/jf960670h.
[36] F. Frauendorfer, P. Schieberle, Changes in Key Aroma Compounds of Criollo Cocoa Beans During Roasting, J. Agric. Food Chem. 56 (2008) 10244–10251.
[37] L. Nicolotti, C. Cordero, C. Cagliero, E. Liberto, B. Sgorbini, P. Rubiolo, C. Bicchi, Quantitative fingerprinting by headspace-Two-dimensional comprehensive gas chromatography-mass spectrometry of solid matrices: Some challenging aspects of the exhaustive assessment of food volatiles, Anal. Chim. Acta. 798 (2013) 115–125. doi:10.1016/j.aca.2013.08.052.
[38] F. Frauendorfer, P. Schieberle, Identification of the Key Aroma Compounds in Cocoa Powder Based on Molecular Sensory Correlations, J. Agric. Food Chem. 54 (2006) 5521–5529.
[39] S.E. Reichenbach, X. Tian, Q. Tao, D.R. Stoll, P.W. Carr, Comprehensive feature analysis for sample classification with comprehensive two-dimensional LC, 33 (2010) 1365–1374. doi:10.1002/jssc.200900859.
[40] P. Schnermann, P. Schieberle, Evaluation of Key Odorants in Milk Chocolate and Cocoa Mass by Aroma Extract Dilution Analyses, J. Agric. Food Chem. 45 (1997) 867–872.
[41] E.J. Kongor, M. Hinneh, D. Van De Walle, O.E. Afoakwa, P. Boeckx, K. Dewettinck, Factors influencing quality variation in cocoa (Theobroma cacao) bean flavour profile — A review, Food Res. Int. 82 (2016) 44–52.
[42] A.C. Aprotosoaie, S.V. Luca, A. Miron, Flavor Chemistry of Cocoa and Cocoa Products — An Overview, Compr. Rev. Food Sci. Food Saf. 15 (2016) 73–91.
[43] L.M. Blumberg, m, (1995).
[44] J. Beens, H.G. Janssen, M. Adahchour, U.A.T. Brinkman, Flow regime at ambient outlet pressure and its influence in comprehensive two-dimensional gas chromatography, J. Chromatogr. A. 1086 (2005) 141–150. doi:10.1016/j.chroma.2005.05.086.
[45] S.E. Reichenbach, D.W. Rempe, Q. Tao, D. Bressanello, E. Liberto, C. Bicchi, S. Balducci, C. Cordero, Alignment for Comprehensive Two-Dimensional Gas Chromatography with Dual Secondary Columns and Detectors, Anal. Chem. 87 (2015) 10056–10063. doi:10.1021/acs.analchem.5b02718.
[46] D.W. Rempe, S.E. Reichenbach, Q. Tao, C. Cordero, W.E. Rathbun, C.A. Zini, Effectiveness of Global, Low-Degree Polynomial Transformations for GCxGC Data Alignment, Anal. Chem. (2016) acs.analchem.6b02254. doi:10.1021/acs.analchem.6b02254.
[47] C.C. Qingping Tao, Chase Heble, Stephen Reichenbach, Interactive tools for optimizing blob detection and template matching for comprehensive two-dimensional chromatography, in: 40th Int. Symp. Capill. Chromatogr. 13th GCxGC Symp. Riva Del Garda Italy May 29 - June 03, 2016, Chromaleont, Messina (Italy), 2016.

Figure Captions:

Figure 1: colorized fuzzy ratio rendering of Chontalpa (Mexico) samples analyzed by TM-GC×GC-MS. *Reference* image corresponds to Chontalpa raw beans; (**1A**) *analyzed* image Roasted beans; (**1B**) *analyzed* image steamed beans; (**1C**) *analyzed* image nibs. For visualization details see text.

Figure 2: TM-GC×GC-MS original method results. Scores plot on the first two principal components (F1-F2 plane), (**2A**) based on the targeted 24 × 132 data matrix (samples × targets) and (**2B**) based on untargeted 24 × 595 data matrix (samples × untargeted *peak-regions*). Samples considered are from Chontalpa, Mexico (Ch), and Ecuador (Ec) at the four processing stages (R, raw; Ro, roasted; St, steamed; N, nibs).

Figure 3: PLS-DA results (**3A**) first 20 most influential variables (cut-off of VIP>1) based on the TM-GC×GC-MS original method fingerprinting and (**3B**) first 20 most influential variables based on the translated FM-GC×2GC-MS/FID fingerprinting. Red bars indicate analytes that were coherently ranked with the first 20 most influential variables for both approaches.

Figure 4: 2D pattern of a roasted Chontalpa sample analyzed with the original method on the loop-type TM platform (**4A**) and with the translated method by reverse-inject FM platform (**4B**). Pink circles indicate the positions of targeted peaks. (**4C**) Illustrates the translated method 2D pattern with the over-imposed untargeted template (green circles indicate *realiable* peaks while red graphics delineate *peak-regions*). (**4D**) shows the 2D pattern from the non translated FM GC×GC-MS method (for chromatographic conditions see Table 1).

Figure 5: Multiple Factor Analysis results (**5A**) correlation between the factors obtained from the first phase of the MFA and those obtained from the second phase comparing the targeted data matrix from the TM and FM methods; (**5B**) displays the coordinates of the projected points in the space resulting from the MFA and illustrates the samples' relative distance on the F1-F2 plane.

Table Captions:

Table 1: Original and translated methods settings, including: columns characteristics, initial head-pressure settings (S/SL injector and EPC), carrier gas (helium) volumetric flows, and linear velocities estimated on the basis of reference equations. Oven temperature programming is also reported. Operative conditions are reported for the non-translated method implemented in the differential flow modulated platform

Table 2: targeted volatiles together with their absolute retention times (^1t_R min and ^2t_R sec), experimental I^T_S, informative role, odor descriptors, Normalized 2D peak volumes from TM GC×GC-MS in Chontalpa (Ch) and Ecuador (Ec) samples (R-raw; Ro-roasted; St-steamed; N-nibs). Information of analytes detection in FM methods is also reported.

Table 1

	Original method settings **GC×GC-MS loop-type thermal modulation**	**GC×2GC-MS/FID reverse-inject differential flow modulation**	**Non-translated method settings** **GC×GC-MS/FID reverse-inject differential flow modulation**
^{1}D Columns	^{1}D: PEG SolGelWax™ (30 m, 0.25mm d_c, 0.25 µm d_f)	^{1}D: PEG SolGelWax™ (10 m, 0.10 mm d_c, 0.10 µm d_f)	^{1}D: PEG SolGelWax™ (30 m, 0.25 mm d_c, 0.25 µm d_f)
^{1}D Carrier gas settings	He carrier @ 1.5 mL/min - constant flow conditions Average velocity ($^1\bar{u}$): 16.61 cm/s Initial head-pressure (relative) 251 kPa Outlet pressure (absolute) 301 kPa Hold-up 3.01 min Outlet velocity 18.007 cm/s	He carrier @ 0.3 mL/min - constant flow conditions Average velocity ($^1\bar{u}$): 12.807 cm/s Initial head-pressure (relative) 470.2 kPa Outlet pressure (absolute) 488.5 kPa Hold-up 1.30 min Outlet velocity 13.868 cm/s	He carrier @ 0.3 mL/min - constant flow conditions Average velocity ($^1\bar{u}$): 3.6558 cm/s Initial head-pressure (relative) 202.02 kPa Outlet pressure (absolute) 292 kPa Hold-up 13.67 min Outlet velocity 3.7124 cm/s
^{2}D Columns	^{2}D: OV1701 (1.0 m, 0.10 mm d_c, 0.10 µm d_f) Loop-capillary: deactivated fused silica (1.0 m, 0.10 mm d_c,)	^{2}D: two parallel columns OV1701 (1.3 m, 0.10 mm d_c, 0.10 µm d_f) Transfer capillary to Tee: deactivated fused silica (5 cm, 0.10 mm d_c,) Split ratio MS/FID: 52:48	^{2}D: OV1701 (5 m, 0.25 mm d_c, 0.3 µm d_f) Transfer capillary to Tee: deactivated fused silica (5 cm, 0.10 mm d_c,) Splitter FID/MS: 0.4, 0.25 d_c toward FID - 0.2, 0.10 d_c toward MS Split ratio MS/FID: 15:85
^{2}D Carrier gas settings	He carrier @ 1.5 mL/min - constant flow conditions Average velocity ($^2\bar{u}$): 172 cm/s Mid-point pressure (relative) 195.3 kPa Hold-up 1.2 s	He carrier @ 12 mL/min (nominal value) - constant flow conditions Average velocity ($^2\bar{u}$): 389 cm/s Initial head-pressure (relative) 387.55 kPa Hold-up 0.6 s	He carrier @ 20 mL/min constant flow conditions Average velocity ($^2\bar{u}$): 342.1 cm/s Initial head-pressure (relative) 191 kPa Hold-up 1.2 s
Bleeding capillary	none	deactivated fused silica: 1.48 m, 0.05 mm d_c,- 0.33 mL/min outlet flow	deactivated fused silica: 0.42 m, 0.05 mm d_c,- 0.33 mL/min outlet flow
Oven Program	40°C(1') to 190°C (10') @ 3°/min		
Modulation	P_M: 3s - Hot-Jet pulse time: 250 ms		
Translated		40°C(0.43') to 190°C @ 6.9373°/min P_M: 2s - Pulse time: 110 ms	
Non-translated		40°C(1') to 190°C @ 3°/min P_M: 4s - Pulse time: 110 ms	50°C(0.5') to 230°C (10') @ 2°/min P_M: 3s - Pulse time: 200 ms

ID	Compound Name	1D (min)	2D (sec)	Exp I^{T}_{S}	Odour descriptor	Ch_R	Ch_Ro	Ch_St	Ch_N	Ec_R	Ec_Ro	Ec_St	Ec_N	Targets FM Translated	Targets FM Not Translated
1	2-Methylpropanal	4.19	0.35	833	green, pungent	1.67	0.00	0.00	0.82	12.47	12.56	0.99	2.19		
2	Methyl acetate	4.59	0.52	853	-	1.39	1.44	0.18	0.95	0.94	0.47	0.23	0.48		
3	2-Methyl tetrahydro-Furan	4.94	0.69	870	-	0.53	0.59	0.60	0.49	0.17	0.16	0.58	0.62		
4	Ethyl Acetate	5.09	0.59	878	fruity, aromatic	53.72	60.37	61.04	64.74	6.66	4.04	4.73	5.40	X	X
5	2-Methyl butanal	5.44	0.64	895	malty	2.59	28.49	37.22	40.74	1.84	18.57	30.17	35.74		X
6	3-Methyl butanal[$]	5.50	0.65	898	malty	12.93	57.41	52.71	53.21	13.67	37.00	46.01	48.29	X	X
7	Ethanol	5.79	0.41	913	ethanol-like	4.71	1.39	2.94	2.55	1.45	3.92	0.61	0.79	X	X
8	2,4,5-Trimethyl-1.3-dioxolane	5.99	0.83	923	-	2.09	2.49	3.59	2.53	0.71	0.28	1.04	1.02		
9	Ethyl propanoate	6.24	0.79	935	-	0.91	1.05	0.82	0.93	0.10	0.08	0.11	0.10		X
10	Ethyl-2-methyl propanoate	6.59	1.03	953	fruity	0.48	0.38	0.42	0.46	0.39	0.31	0.40	0.40		X
11	2,3-Butanedione[£]	6.64	0.55	955	buttery	8.02	3.39	1.80	2.02	10.80	3.18	3.95	5.30		X
12	2-Pentanone	6.69	0.79	958	fruity	5.59	7.33	7.71	6.67	8.15	5.20	4.29	4.28	X	X
13	Pentanal	6.84	0.79	965	almond, pungent, malty	0.00	0.00	0.00	0.03	0.00	1.20	0.00	0.00		
14	1-Methyl propyl acetate	6.84	1.03	966	-	0.76	0.85	0.86	0.96	0.54	0.57	0.46	0.37	X	X
15	2-Methyl propyl acetate	7.49	1.00	998	-	11.65	13.85	15.40	11.73	5.23	5.22	5.19	4.38	X	X
16	2-Butanol	7.60	0.55	1001	winey	2.86	2.86	2.98	2.13	3.26	3.98	3.76	3.59	X	X
17	α-Pinene	7.69	1.93	1005	harsh, terpene-like	0.16	0.15	0.14	0.13	0.30	0.26	0.22	0.25		X
18	2-Ethyl-5-methyl-furan	7.89	1.00	1012	-	1.34	1.45	1.34	1.10	2.19	1.76	3.23	2.13		X
19	Ethyl butanoate	7.99	1.21	1016	sweet, fruity	1.14	1.73	1.27	1.24	0.39	0.38	0.54	0.34		X
20	2-Methyl-3-Buten-2-ol	8.19	1.24	1022	-	1.66	1.90	1.63	1.59	3.11	2.89	2.69	3.36		
21	Ethyl-2-methyl butanoate[$]	8.54	1.41	1035	fruity	1.26	1.23	1.02	0.91	1.28	0.97	1.10	0.94	X	X
22	2,3-Pentandione[£]	8.74	0.76	1041	caramel	0.24	1.60	0.78	0.86	0.29	2.25	0.62	0.65		X
23	Ethyl-3-methyl butanoate	8.99	1.38	1050	fruity	0.72	0.32	0.71	0.49	0.67	0.30	0.87	0.55		X
24	Dimethyl disulfide[£]	9.13	0.83	1055	sulfurous	0.52	0.00	0.00	1.16	0.59	0.00	0.00	0.00		
25	2-pentanol acetate	9.15	1.38	1056	-	1.35	1.49	1.14	0.95	0.73	0.87	0.76	0.65	X	X
26	Butyl acetate	9.19	1.14	1057	fruity, herbaceous	0.73	0.86	0.71	0.61	0.49	0.55	0.47	0.44		X
27	Hexanal	9.54	1.14	1069	tallowy, leaf-like	0.44	0.81	0.64	0.55	2.54	2.64	1.43	1.19		X
28	2-Methyl-1-propanol	9.69	0.59	1074	-	1.22	1.89	1.46	1.20	1.90	0.95	1.28	1.06	X	X
29	2-Methyl-2-butenal	10.04	0.86	1086	-	0.47	0.81	0.88	0.80	0.90	1.12	1.41	1.65		X
30	2-Pentanol	10.74	0.69	1108	light, seedy, sharp	10.48	17.83	14.26	11.50	16.85	12.78	11.18	9.31	X	X
31	1-Butanol-3-methyl-acetate	10.89	1.38	1112	-	80.45	84.02	84.56	67.61	41.74	40.46	38.40	31.45	X	X
32	Ethyl pentanoate	11.01	1.39	1115	fruity, sweet	0.18	0.14	0.14	0.00	0.00	0.00	0.00	0.00		X
33	Butyl-2-methyl propanoate	11.19	1.83	1120	fruity, sweet	0.19	0.24	0.12	0.15	0.06	0.05	0.05	0.10		X
34	4-Methyl-3-penten-2-one	11.29	1.00	1123	-	0.42	0.80	0.86	0.72	0.45	0.69	1.37	1.13		
35	1-Butanol	11.64	0.59	1132	winey	3.50	2.30	1.95	2.23	2.75	4.83	1.74	2.36	X	X
36	β-Myrcene	12.24	1.83	1148	-	0.61	0.55	0.69	0.65	5.87	9.11	10.81	8.35		X
37	1-Pentyl acetate	12.79	1.41	1163	fruity, metallic, green	1.40	1.51	1.14	0.95	0.74	0.88	0.76	0.64	X	X
38	2-Heptanone	13.19	1.38	1173	sweet, fruity	2.33	2.80	2.40	2.05	26.90	45.85	26.81	20.34	X	X
39	2-Ethyl hexanal	13.39	1.76	1179	-	1.38	1.39	1.20	1.01	2.25	2.26	1.75	1.87		X
40	Limonene	13.74	1.93	1188	citrus, mint	1.29	1.19	1.56	1.71	1.47	2.04	2.04	2.71	X	X
41	2-Methyl-1-butanol	14.19	0.66	1200	fermented, fatty	12.90	10.95	11.10	10.48	15.94	14.93	10.68	10.39		X
42	Pyrazine	14.39	0.75	1205	earthy	0.00	0.00	0.00	0.00	0.00	0.09	0.00	0.29		X
43	Butyl butanoate	14.64	1.86	1211	fruity, flowery, sweet	31.81	35.89	25.74	23.93	66.83	65.58	55.92	59.00	X	X

44	2-Hexanol	14.69	0.83	1212	mushroom, green	0.33	0.39	0.46	0.43	0.87	0.89	0.78	0.59		X
45	Ethyl hexanoate	14.94	1.74	1219	fruity	5.39	5.69	4.70	3.97	0.00	0.00	0.00	0.00	X	X
46	2-Pentylfuran	15.09	1.52	1222	buttery, green beans	0.80	1.46	1.33	1.11	0.47	0.55	2.00	1.20	X	X
47	Ethyl tiglate	15.39	1.31	1229	-	0.32	0.32	0.30	0.26	0.21	0.27	0.26	0.25		
48	1-Pentanol	15.89	0.69	1241	sweet, pungent	0.75	0.87	0.57	0.65	1.27	1.34	0.91	1.01		X
49	2,4-Dimethyl-3-pentanol	16.34	0.66	1252	-	0.17	0.15	0.12	0.13	0.26	0.43	0.30	0.32		
50	Methyl pyrazine[£]	16.69	0.79	1260	earthy	0.86	3.26	6.09	5.87	0.62	2.39	8.54	7.63	X	X
51	Hexyl acetate	16.89	1.62	1265	fruity	2.44	3.83	2.36	2.15	0.31	0.38	0.40	0.34	X	X
52	3-Hydroxy-2-butanone[£]	17.24	0.62	1274	buttery	10.95	11.94	14.08	16.73	25.77	27.89	32.32	26.54	X	X
53	2-Octanone	17.49	1.55	1280	mould, green	0.30	0.41	0.39	0.35	0.57	1.01	0.74	0.58		X
54	Octanal	17.64	1.59	1283	fatty, sharp	0.15	0.23	0.18	0.19	0.28	0.31	0.33	0.23		
55	1-Hydroxy-2-propanone[£]	17.94	0.52	1290	buttery	0.68	3.46	2.44	2.70	1.10	4.92	7.34	9.03	X	X
56	2-Methyl-1-pentanol	17.99	0.76	1292	-	0.08	0.09	0.09	0.10	0.28	0.39	0.31	0.32		X
57	2-Ethyl-(E)-2-hexenal	18.04	1.59	1293	-	3.51	3.78	3.26	3.09	6.19	6.43	5.79	6.07	X	X
58	3-Hepten-2-one	18.09	1.56	1294	-	0.20	0.28	0.26	0.26	0.27	1.12	0.94	0.87		
59	2-Heptanol[$]	18.94	0.90	1314	citrusy	1.75	5.07	8.19	8.34	18.10	37.96	25.66	23.85	X	X
60	2,3-Octanedione[£]	19.14	1.28	1319	-	0.30	0.40	0.33	0.36	0.31	0.61	0.59	0.58		X
61	2,5-Dimethyl pyrazine[£]	19.24	0.88	1321	earthy	0.26	0.50	2.50	2.55	0.00	2.99	5.82	4.18	X	X
62	2,6-Dimethyl pyrazine[£]	19.34	0.90	1324	earthy	0.98	4.60	8.11	7.88	1.00	3.20	8.94	7.44	X	X
63	Ethyl pyrazine[£]	19.54	0.89	1328	earthy	0.00	1.69	0.00	1.15	0.00	0.00	0.00	0.00		X
64	6-Methyl-5-hepten-2-one	19.64	1.28	1331	pungent, green	0.20	0.21	0.17	0.16	0.39	0.47	0.52	0.46		X
65	2,3-Dimethyl pyrazine[£]	20.09	0.93	1341	earthy	5.22	7.85	11.04	10.92	4.25	7.46	9.71	8.01	X	X
66	1-Hexanol	20.29	0.79	1346		0.41	0.59	0.62	0.52	0.91	0.80	0.75	0.73		X
67	4-Hydroxy-4-methyl-2-pentanone	20.54	0.83	1352	fruity, banana, soft	1.34	1.91	1.18	1.35	1.39	1.24	1.23	1.44		
68	Dimethyl trisulfide[$]	21.24	1.03	1368	sulfury, cabbage	0.18	0.69	1.55	1.22	0.27	0.45	2.57	2.35	X	X
69	2-Ethyl-6-methyl pyrazine[£]	21.74	1.07	1380	earthy	0.17	1.24	2.72	2.74	0.16	0.47	1.86	1.52	X	X
70	2-Nonanone	21.94	1.72	1385	-	0.98	0.99	1.07	1.06	7.01	14.81	6.68	7.95	X	X
71	2-Ethyl-5-methyl pyrazine[£]	22.04	1.07	1387	earthy	0.20	0.87	2.52	2.42	0.23	0.52	2.61	2.12	X	X
72	Nonanal	22.14	1.72	1389	fatty, waxy, pungent	0.55	0.66	0.61	0.63	0.70	1.18	1.45	1.19	X	
73	2,3,5-Trimethylpyrazine[$]	22.64	1.03	1401	earthy	13.51	20.54	29.40	29.01	4.45	15.04	25.93	17.74	X	X
74	*α-Thujone (ISTD)*	*23.19*	*1.79*	*1414*	-	*100.00*	*100.00*	*100.00*	*100.00*	*100.00*	*100.00*	*100.00*	*100.00*	*X*	*X*
75	2-Octanol	23.49	1.07	1422	mushroom, fatty, creamy	0.15	0.26	0.32	0.27	0.08	0.15	0.53	0.34		
76	Ethyl octanoate	23.89	2.00	1431	-	5.90	4.80	5.64	5.30	1.64	1.51	1.94	1.58	X	X
77	1-Octen-3-ol	23.94	0.64	1433	mould, earthy	0.075	0.071	0.07	0.85	0.06	0.08	0.09	0.05		
78	Acetic acid[$]	23.99	0.57	1434	sour, vinegary	671.50	678.79	710.90	718.07	412.61	394.87	448.73	432.71	X	X
79	2-Ethyl-3,6-dimethyl pyrazine[£]	24.29	1.20	1441	earthy	0.00	0.80	0.00	0.00	0.00	0.00	0.00	0.00	X	X
80	Furfural[£]	24.88	0.69	1455	sweet, bread-like	0.27	2.42	2.74	2.75	2.04	7.04	3.60	2.30	X	X
81	1-Acetyloxy-2-propanone[£]	24.89	1.31	1455	-	0.91	3.05	3.75	3.66	2.45	7.41	7.33	5.75		X
82	2-Ethyl-3,5-dimethyl-pyrazine[$]	24.94	1.17	1457	earthy	1.66	3.35	5.32	5.41	0.53	1.32	3.73	2.55	X	X
83	Trans-linalool oxide	25.29	1.21	1465	sweet floral, citrus, fruity	1.27	1.52	1.35	1.37	2.12	3.64	3.11	3.49	X	X
84	2,6-Dimethyl-4-heptanol	25.44	1.40	1469	-	0.00	0.00	0.00	0.00	0.00	0.00	0.21	0.17		
85	Tetramethyl pyrazine[£]	25.54	1.14	1471	earthy	74.82	81.16	72.64	78.72	25.73	62.40	80.90	51.75	X	X
86	2,3-Butanedioldiacetate	25.99	1.14	1482	-	18.19	15.42	15.82	13.47	0.89	1.01	1.32	0.94	X	X
87	2-Ethyl-1-hexanol	26.04	0.97	1483	-	2.26	2.91	2.99	2.80	4.06	4.10	4.35	4.31	X	X

88	Decanal	26.54	1.86	1495	sweet, waxy	0.57	0.80	0.65	0.93	0.49	0.53	0.55	0.53		
89	2-Acetyl furane	26.64	0.72	1498	-	0.51	1.34	2.41	2.17	0.32	0.78	4.24	4.19	X	X
90	3,5-Diethyl-2-methyl pyrazine[$]	27.09	0.55	1509	earthy	0.90	2.65	4.77	4.73	0.28	0.91	2.42	1.60	X	X
91	Benzaldehyde	27.34	0.79	1515	almond, burnt sugar	68.97	68.13	54.21	53.63	37.50	36.17	34.53	33.10	X	X
92	2,3-Butanediol-diacetate	27.49	1.10	1519	-	11.39	9.14	8.65	8.01	0.87	1.17	1.13	0.94	X	X
93	Furfuryl acetate	27.79	0.79	1526	-	0.71	0.75	0.90	0.82	0.40	0.49	1.09	1.09		X
94	2-Nonanol	27.83	0.94	1527	-	0.00	0.00	0.00	0.06	0.20	0.07	0.00	0.00		
95	2,3-Butanediol	27.99	0.55	1531	-	96.74	95.24	121.63	124.30	63.90	55.03	56.18	53.06	X	X
96	Propanoic acid	27.99	0.40	1531	fruity, pungent	2.31	0.00	3.21	4.94	1.15	0.83	6.25	5.10		X
97	Linalool	28.44	1.00	1542	citrus	0.69	0.62	0.67	0.70	5.08	10.31	12.65	7.62	X	X
98	1-Octanol	28.84	0.93	1552	moss, nut, mushroom	1.14	1.23	1.04	1.46	0.60	0.70	1.03	0.91	X	X
99	2-Methyl propanoic acid[$]	29.09	0.48	1558	rancid	24.40	22.65	20.52	20.89	27.82	17.68	22.04	21.74	X	X
100	2,3-Butanediol	29.44	0.52	1567	-	143.17	129.71	161.58	164.03	103.07	93.20	94.97	96.28	X	X
101	Dihydro-2(3H)-furanone	31.34	0.76	1614	-	8.25	9.26	10.74	10.24	13.15	11.65	14.75	14.60	X	X
102	Butanoic acid[$]	31.54	0.48	1619	sweaty, rancid	10.43	6.90	8.52	8.90	4.94	3.76	6.66	5.35	X	X
103	Phenyl acetaldehyde[$]	32.04	0.83	1632	honey-like	2.02	1.31	1.94	1.62	1.06	1.07	2.71	2.11		X
104	Ethyl decanoate	32.14	2.31	1635	fruity	0.91	0.88	1.00	1.18	0.41	0.40	0.46	0.42		
105	Acetophenone	32.34	0.86	1640	-	10.32	11.97	10.96	10.56	4.80	6.21	6.66	5.95	X	X
106	2-Furan methanol[£]	32.59	0.52	1646	burned	4.81	10.68	13.91	13.56	3.18	6.84	26.42	27.98	X	X
107	Ethyl benzoate	33.04	1.49	1658	-	0.00	0.75	0.93	0.81	0.00	0.00	0.00	0.00		X
108	3-Methyl butanoic acid[$]	33.09	0.52	1659	rancid	79.24	70.91	70.68	71.33	81.95	65.22	82.51	70.83	X	X
109	Dodecanal	34.94	2.01	1707	fatty, citrus-like	0.13	0.21	0.00	0.00	0.00	0.00	0.00	0.00		
110	Pentanoic acid	35.94	0.46	1734	sweaty	0.88	0.66	0.90	0.83	0.72	1.67	1.01	1.19	X	X
111	4-Ethyl phenyl acetate	37.39	1.03	1773	-	2.30	2.32	2.60	2.63	0.44	0.50	0.57	0.48		
112	4-Methyl pentanoic acid	38.19	0.52	1795	-	1.93	1.80	2.53	2.48	0.87	1.04	2.60	2.05	X	
113	1-Phenyl ethanol	38.24	0.63	1796	-	1.71	0.78	1.03	0.83	1.15	1.11	0.37	0.00	X	X
114	2-Phenyl-ethyl acetate[$]	38.39	0.62	1800	flowery	25.71	29.50	28.23	31.26	5.07	5.50	5.80	4.81	X	X
115	Hexanoic acid	39.69	0.52	1837	rancid	5.25	4.35	5.43	5.42	5.99	10.76	7.37	4.31	X	X
116	Ethyl dodecanoate	39.74	2.48	1838	-	1.49	1.43	1.57	2.00	0.58	0.66	0.66	0.59		
117	Guaiacol	39.84	0.75	1841	spicy	1.05	0.00	0.67	0.00	0.00	0.00	0.00	0.00	X	X
118	2-Methylpropyl benzoate	40.19	1.21	1851	-	13.27	14.10	17.86	16.67	15.90	17.61	16.81	16.82	X	X
119	Benzyl alcohol	40.44	0.59	1858	sweet, fruity	3.59	3.08	3.52	3.82	3.09	2.28	3.16	2.91	X	X
120	Phenyl ethyl Alcohol[$]	41.64	0.66	1892	honey-like	40.30	37.40	38.28	42.44	34.79	38.30	33.17	32.45	X	X
121	(E)-2-Phenyl-2-butenal[£]	42.44	0.97	1915	-	1.02	3.89	3.86	4.65	0.60	1.55	1.57	1.53	X	X
122	Acetyl pyrrole	43.64	0.59	1950	popcorn-like	2.58	7.65	11.24	11.92	1.81	5.33	11.85	10.01	X	X
123	Phenol	44.74	0.52	1982	-	1.14	1.04	1.43	1.43	0.57	0.54	1.25	1.10	X	X
124	1H-Pyrrole-2-carboxaldehyde	45.34	0.52	2000	-	0.72	1.00	1.76	1.47	1.24	1.47	4.34	4.73	X	X
125	4-Hydroxy-2,5-dimethyl-3(2H)-furanone[£]	45.64	0.59	2009	caramel-like	1.06	1.93	3.32	3.85	0.85	1.83	3.25	2.61	X	X
126	Octanoic acid	46.94	0.55	2049	sweaty	1.84	2.11	2.47	2.88	4.65	7.48	2.98	1.77		X
127	5-Methyl-2-phenyl-2(Z)-hexenal	47.24	1.21	2058	-	0.40	2.02	2.41	3.23	0.42	2.17	0.79	0.73	X	X
128	Nonanoic acid	50.34	0.57	2156	sweaty, waxy	0.41	1.34	0.43	0.36	0.58	0.00	0.67	2.04		
129	2,3-Dihydro-3,5-dihydroxy-6-methyl-4H-pyran-4-one	52.74	0.48	2234	-	0.26	10.07	10.59	16.77	0.49	7.16	7.28	6.24		
130	Decanoic acid	53.49	0.66	2259	soap-like, fatty	0.73	0.72	0.96	0.99	1.70	1.14	2.70	0.89	X	X

131	1(3H)-Isobenzofuranone	55.39	0.69	2330	-	8.69	8.59	10.13	9.65	9.10	10.15	9.67	9.32	X	
132	2-Phenyl acetic acid	59.44	0.79	2549	honey-like	3.14	0.60	4.80	4.94	0.97	1.17	2.18	1.08		
	Total Number of Targets (ISTD)					**123 (1)**	**122 (1)**	**122 (1)**	**125 (1)**	**120 (1)**	**121 (1)**	**120 (1)**	**120 (1)**	**74 (1)**	**103 (1)**

Figure 1

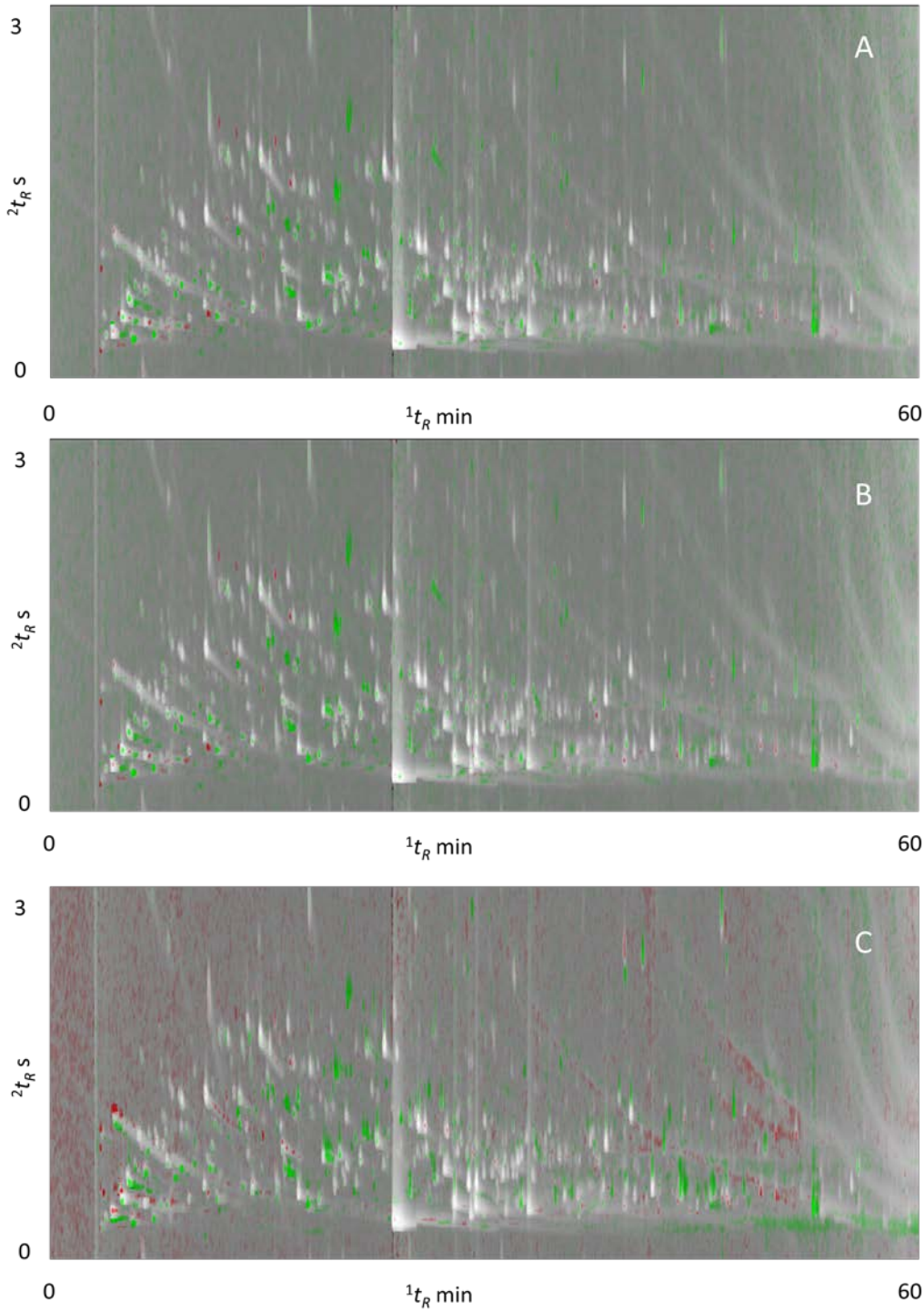

Figure 2

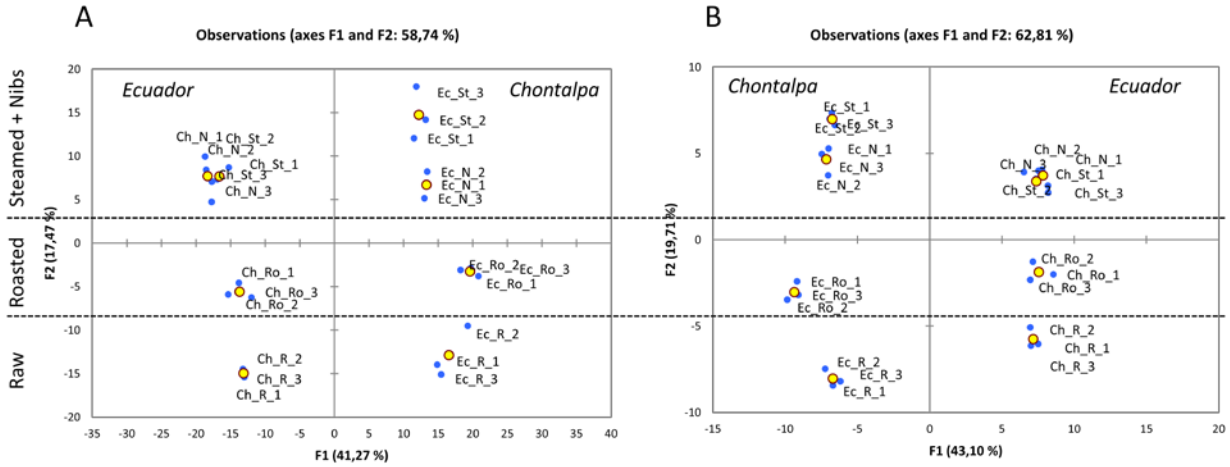
A
Observations (axes F1 and F2: 58,74 %)
Ecuador
Chontalpa
Steamed + Nibs
Roasted
Raw
F2 (17,47 %)
F1 (41,27 %)
B
Observations (axes F1 and F2: 62,81 %)
Chontalpa
Ecuador
F2 (19,71 %)
F1 (43,10 %)

Figure 3

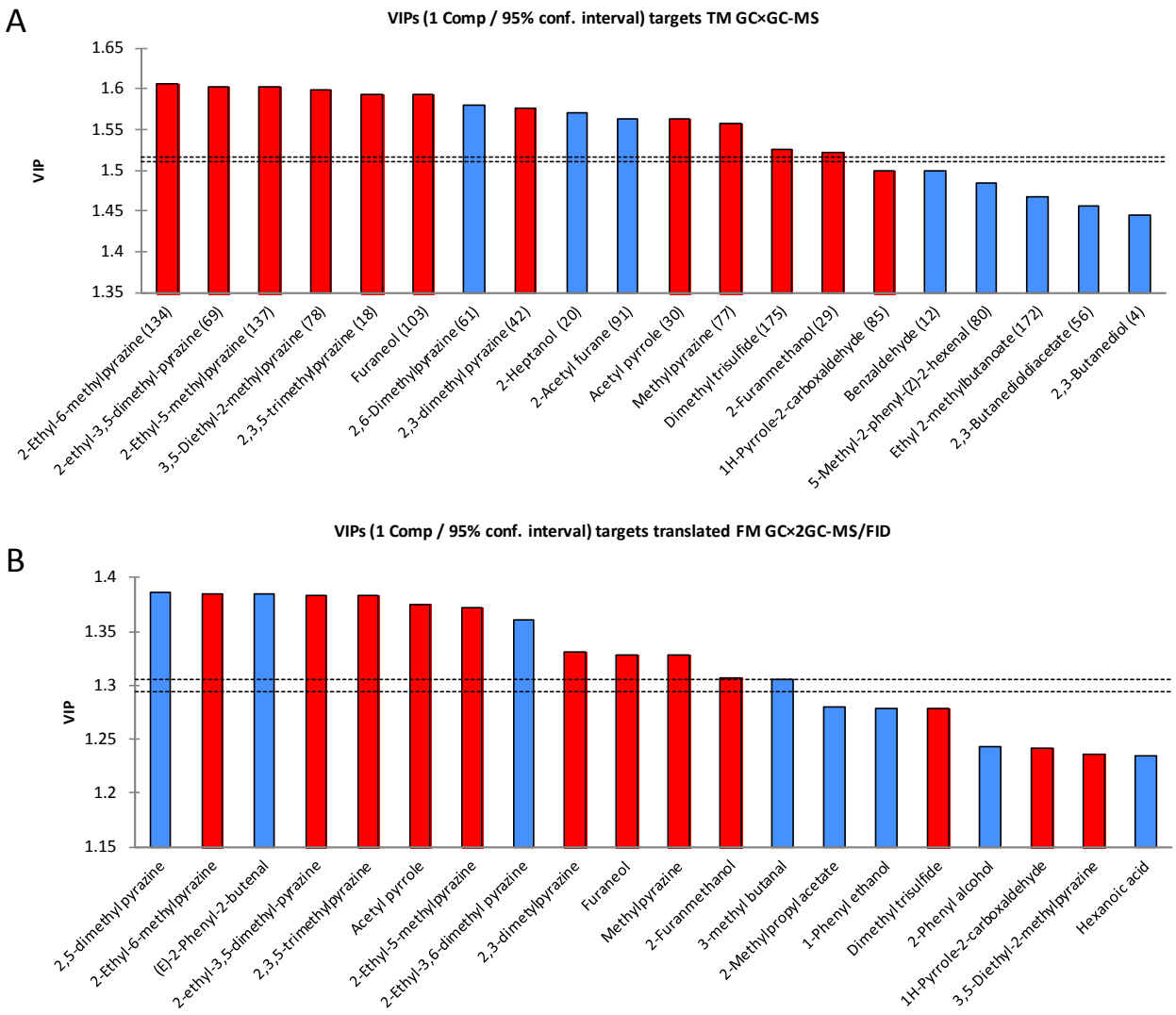
A
VIPs (1 Comp / 95% conf. interval) targets TM GC×GC-MS
VIP
1.65
1.6
1.55
1.5
1.45
1.4
1.35
2-Ethyl-6-methylpyrazine (134)
2-ethyl-3,5-dimethyl-pyrazine (69)
2-Ethyl-5-methylpyrazine (137)
3,5-Diethyl-2-methylpyrazine (78)
2,3,5-trimethylpyrazine (18)
Furaneol (103)
2,6-Dimethylpyrazine (61)
2,3-dimethyl pyrazine (42)
2-Heptanol (20)
2-Acetyl furane (91)
Acetyl pyrrole (30)
Methylpyrazine (77)
Dimethyl trisulfide (175)
2-Furanmethanol (29)
1H-Pyrrole-2-carboxaldehyde (85)
Benzaldehyde (12)
5-Methyl-2-phenyl-(Z)-2-hexenal (80)
Ethyl 2-methylbutanoate (172)
2,3-Butanedioldiacetate (56)
2,3-Butanediol (4)
B
VIPs (1 Comp / 95% conf. interval) targets translated FM GC×2GC-MS/FID
VIP
1.4
1.35
1.3
1.25
1.2
1.15
2,5-dimethyl pyrazine
2-Ethyl-6-methylpyrazine
(E)-2-Phenyl-2-butenal
2-ethyl-3,5-dimethyl-pyrazine
2,3,5-trimethylpyrazine
Acetyl pyrrole
2-Ethyl-5-methylpyrazine
2-Ethyl-3,6-dimethyl pyrazine
2,3-dimetylpyrazine
Furaneol
Methylpyrazine
2-Furanmethanol
3-methyl butanal
2-Methylpropyl acetate
1-Phenyl ethanol
Dimethyl trisulfide
2-Phenyl alcohol
1H-Pyrrole-2-carboxaldehyde
3,5-Diethyl-2-methylpyrazine
Hexanoic acid

Figure 4

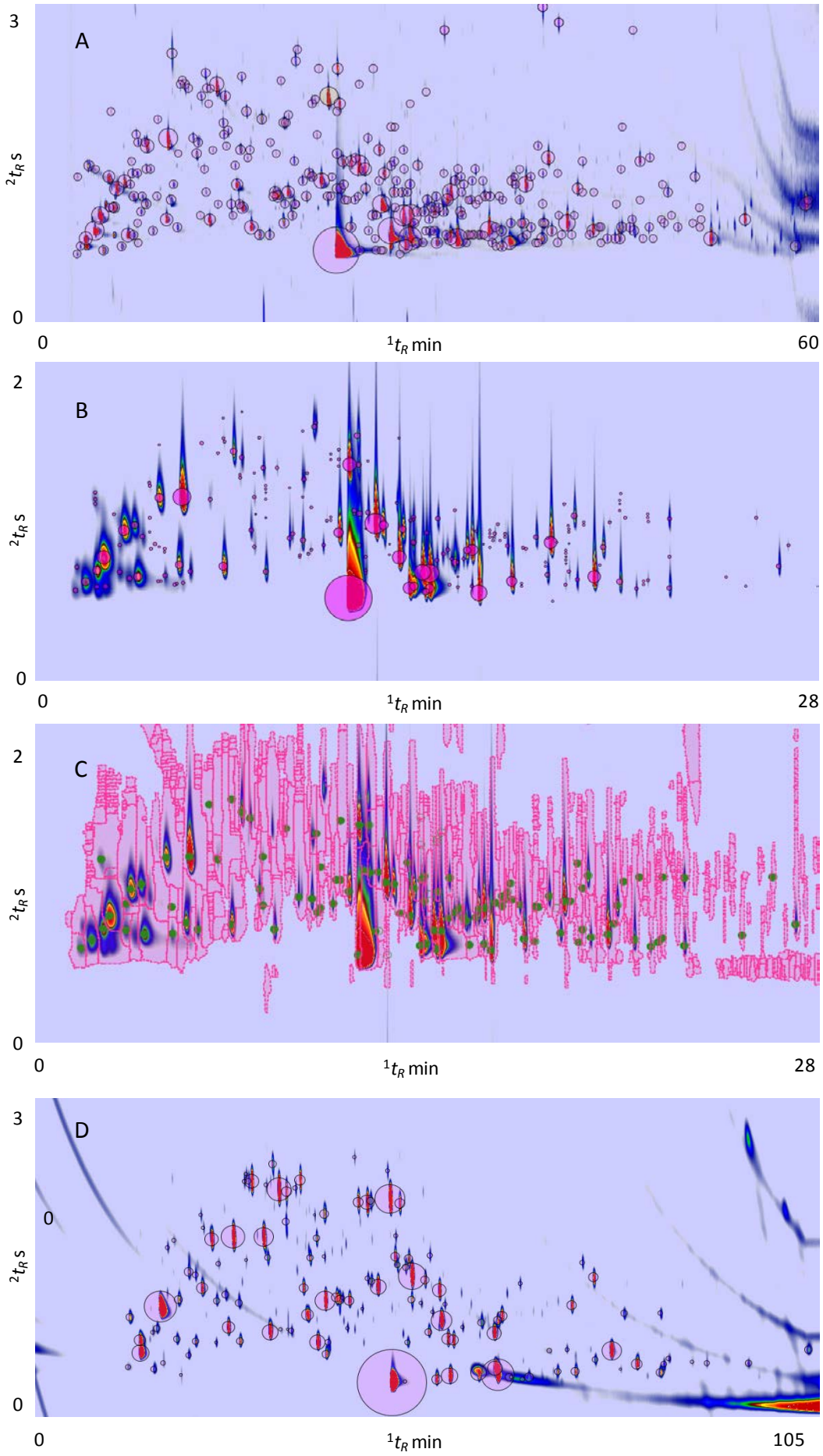
A
3
0
^2t_R s
0
^1t_R min
60
B
2
0
^2t_R s
0
^1t_R min
28
C
2
0
^2t_R s
0
^1t_R min
28
D
3
0
0
^2t_R s
0
^1t_R min
105

Figure 5

A

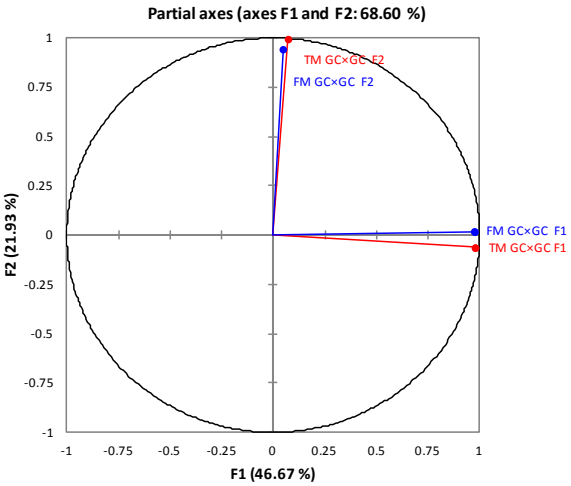
Partial axes (axes F1 and F2: 68.60 %)
TM GC×GC F2
FM GC×GC F2
FM GC×GC F1
TM GC×GC F1
F2 (21.93 %)
F1 (46.67 %)
1
0.75
0.5
0.25
0
-0.25
-0.5
-0.75
-1
-1
-0.75
-0.5
-0.25
0
0.25
0.5
0.75
1

B

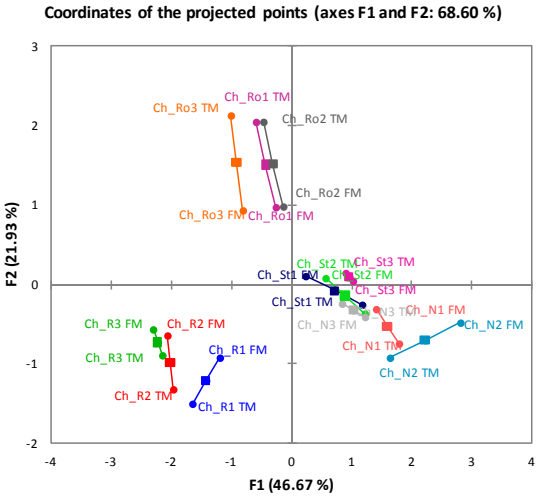
Coordinates of the projected points (axes F1 and F2: 68.60 %)
Ch_Ro1 TM
Ch_Ro3 TM
Ch_Ro2 TM
Ch_Ro2 FM
Ch_Ro3 FM
Ch_Ro1 FM
Ch_St2 TM
Ch_St3 TM
Ch_St1 TM
Ch_St2 FM
Ch_St3 FM
Ch_St1 TM
Ch_N1 FM
Ch_N3 TM
Ch_N3 FM
Ch_N2 FM
Ch_N1 TM
Ch_N2 TM
Ch_R3 FM
Ch_R2 FM
Ch_R1 FM
Ch_R3 TM
Ch_R2 TM
Ch_R1 TM
F2 (21.93 %)
F1 (46.67 %)
3
2
1
0
-1
-2
-4
-3
-2
-1
0
1
2
3
4